The EMBO Journal (2011) 30, 4712–4727 | © 2011 European Molecular Biology Organization | All Rights Reserved 0261-4189/11
www.embojournal.org

THE EMBO JOURNAL

Regulation of integrin affinity on cell surfaces

Thomas Schürpf and Timothy A Springer*

Department of Pathology, Harvard Medical School, Immune Disease Institute and Children's Hospital, Boston, MA, USA

Lymphocyte activation triggers adhesiveness of lymphocyte function-associated antigen-1 (LFA-1; integrin $\alpha_L\beta_2$) for intercellular adhesion molecules (ICAMs) on endothelia or antigen-presenting cells. Whether the activation signal, after transmission through multiple domains to the ligand-binding αI domain, results in affinity changes for ligand has been hotly debated. Here, we present the first comprehensive measurements of LFA-1 affinities on T lymphocytes for ICAM-1 under a broad array of activating conditions. Only a modest increase in affinity for soluble ligand was detected after activation by chemokine or T-cell receptor ligation, conditions that primed LFA-1 and robustly induced lymphocyte adhesion to ICAM-1 substrates. By stabilizing well-defined LFA-1 conformations by Fab, we demonstrate the absolute requirement of the open LFA-1 headpiece for adhesiveness and high affinity. Interaction of primed LFA-1 with immobilized but not soluble ICAM-1 triggers energy-dependent affinity maturation of LFA-1 to an adhesive, high affinity state. Our results lend support to the traction or translational motion dependence of integrin activation.

The EMBO Journal (2011) **30,** 4712–4727. doi:10.1038/emboj.2011.333; Published online 23 September 2011
Subject Categories: cell & tissue architecture
Keywords: ICAM-1; CD11a/CD18; lymphocyte function-associated antigen-1 (LFA-1); metal ion-dependent adhesion site (MIDAS); stromal cell-derived factor (SDF)

Introduction

Leukocyte function-associated antigen-1 (LFA-1) is one of the best-studied members of the integrin family of adhesion receptors. It is a type I transmembrane (TM) α/β heterodimeric protein consisting of the α_L subunit, which carries the ligand-binding αI domain, and the noncovalently associated β_2 subunit (Humphries, 2000; Luo *et al*, 2007). The two subunits form a large 13-domain extracellular portion and two short cytoplasmic tails (Figure 1). LFA-1 is expressed on all leukocytes, mediates firm adhesion to and extravasation through endothelium upon activation, and forms part of the immunological synapse between a lymphocyte and an antigen-presenting cell (Grakoui *et al*, 1999). Interaction with an opposing cell is mediated by binding the intercellular adhesion molecules, ICAM-1, -2, -3, and -5. Among these ligands ICAM-1 has the highest affinity for the α_L I domain (Shimaoka *et al*, 2001). LFA-1-dependent cell adhesion requires an activating signal, for example, chemokine binding or T-cell receptor (TCR) ligation (Dustin and Springer, 1989; Shamri *et al*, 2005). LFA-1 transmits signals across the cell membrane in a bidirectional fashion. Intracellular signalling pathways induce separation of the cytoplasmic tails and activation of the LFA-1 ectodomain in inside–out signalling (Kim *et al*, 2003), while binding to multivalent ligand induces clustering and outside–in signalling (Kim *et al*, 2004).

What molecular properties allow LFA-1 to transmit signals in such a sophisticated manner across the membrane and across multiple extracellular domain boundaries (Figure 1)? Ever since T lymphocyte adhesiveness was found to be transiently activated by TCR crosslinking with no concomitant change in cell surface expression, conformational changes in the LFA-1 ligand-binding site have been postulated (Dustin and Springer, 1989). A number of structural studies in recent years have provided better understanding of how signals may be transmitted from the intracellular integrin domains across the cell membrane to the ligand-binding domain (Luo *et al*, 2007). LFA-1 has an integrin headpiece with the ligand-binding α_L I domain at its tip and two legs that connect to the membrane (Figure 1). Resting integrins have low affinity for ligand and adopt a bent conformation in which the headpiece contacts the leg and buries a large, $>4000\,Å^2$ interface (Xiong *et al*, 2001; Takagi *et al*, 2002; Xie *et al*, 2010) (Figure 1A). Multiple signalling and cytoskeletal proteins including talin, kindlins, α-actinin, filamin, and 14-3-3 proteins bind to the intracellular β subunit tails and connect integrins with the cytoskeleton (Gahmberg *et al*, 2009; Moser *et al*, 2009). Activation of LFA-1 by the talin head domain induces separation of the cytoplasmic tails and the TM domains (Kim *et al*, 2003), which is thought to destabilize the headpiece–leg interface on the extracellular side and trigger integrin extension (Figure 1A and B). In a separate conformational movement termed headpiece opening, the α and β leg knees separate by 70 Å and the β_2 hybrid domain swings out (Figure 1B and C) (Xiao *et al*, 2004). Hybrid domain swing out is linked to the β_2 I domain by pulling down the βI α7-helix in a piston-like motion (Figure 1B and C). Integrin extension, headpiece opening, and β_2 I domain activation can be detected or induced by monoclonal antibody binding to distinct activation epitopes (Drbal *et al*, 2001; Lu *et al*, 2001a; Shamri *et al*, 2005; Nishida *et al*, 2006; Stanley *et al*, 2008; Chen *et al*, 2010; Xie *et al*, 2010). β_2 I domain activation is thought to be relayed to the αI domain by binding of the metal ion-dependent adhesion site (MIDAS) of the β_2 I domain to α_L-Glu-310, at the end of the C-terminal α7-helix in the α_L I domain (Luo *et al*, 2007) (Figure 1C). Crystal structures showed that this αI α7-helix allosterically regulates αI domain conformation by moving downwards along its axis. Locking the α7-helix at various positions by engineered disulphide bonds induced a closed, intermediate, or open I domain conformation (Shimaoka *et al*, 2003b). The locked closed I domain conformation corresponds to the

*Corresponding author. Department of Pathology, Harvard Medical School, Immune Disease Institute and Children's Hospital, 3 Blackfan Circle, Boston, MA 02115, USA. Tel.: +1 617 713 8200; Fax: +1 617 713 8232; E-mail: springer@idi.harvard.edu

Received: 25 May 2011; accepted: 22 August 2011; published online: 23 September 2011

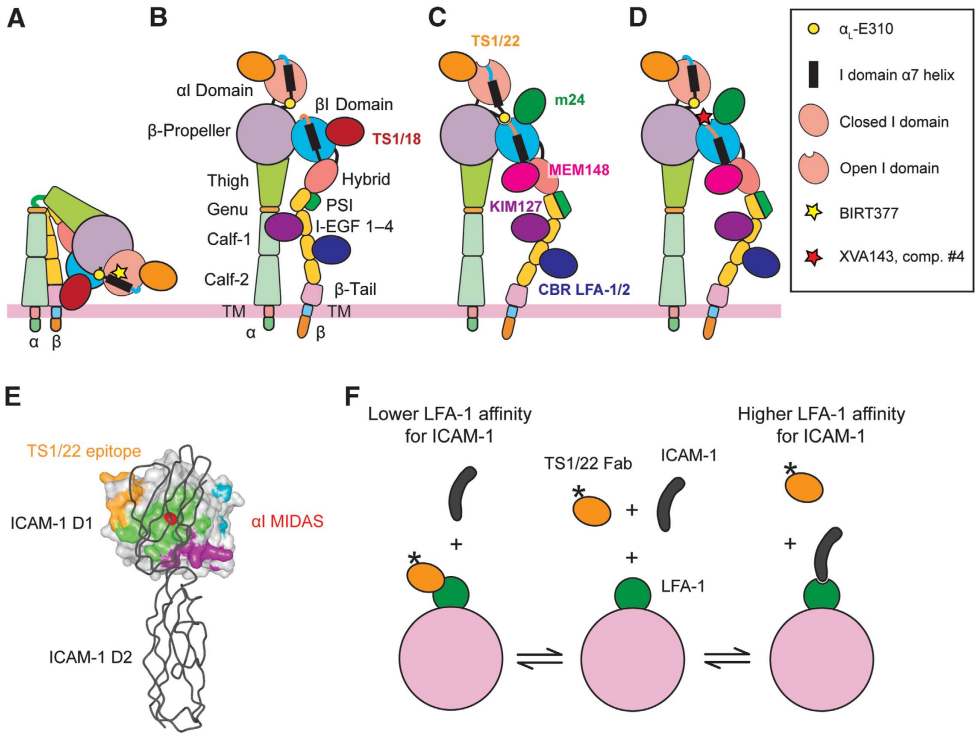

Figure 1 Integrin activation states and competition binding assay schematic. (**A**–**D**) Integrin activation states. Fab and small molecule inhibitors used in this study are shown. Fabs are shown bound to all integrin conformations they bind, and small molecules are shown with conformations that they stabilize. (**A**) An inactive integrin in a bent conformation. (**B**) Disruption of TM domain association induces an extended conformation with a closed headpiece. (**C**) After extension, the hybrid domain can swing out in the open integrin headpiece with an active βI domain, which is suggested to pull down the αI domain α7 helix by binding of α_L-E310 to the β_2 MIDAS. (**D**) The α/β I allosteric class of integrin inhibitors are believed to ligate the βI domain and induce integrin extension and the open headpiece, but to block activation of the αI domain. (**E**) Basis for competition binding assay, based on the crystal structure of the α_L I domain bound to ICAM-1 domains 1 and 2 (Shimaoka *et al*, 2003b). The LFA-1 I domain is depicted as a molecular surface in grey. Species-specific residues in the TS1/22 epitope are coloured in orange. The ligand-binding MIDAS Mg^{2+} is in red and ICAM-1-binding surface is in green. Binding of ICAM-1 (grey Cα trace) is sterically hindered by TS1/22 binding. Taken from Lu *et al* (2004). (**F**) Schematic of the competition binding assay. Radiolabelled TS1/22 Fab at a fixed concentration and varying concentrations of Hi3-ICAM-1 are mixed with LFA-1-expressing cells. After equilibrium binding is reached, cells are pelleted through an oil cushion and bound radioactivity is measured.

wild-type (wt), low affinity conformation, whereas the locked intermediate and open I domain conformations had 500-fold and 10 000-fold increased affinity for ICAM-1, respectively (Shimaoka *et al*, 2003b).

Despite information on structural rearrangements using purified integrins and their fragments (Lee *et al*, 1995; Emsley *et al*, 2000; Beglova *et al*, 2002; Takagi *et al*, 2002; Shimaoka *et al*, 2003b; Shi *et al*, 2005; Nishida *et al*, 2006; Chen *et al*, 2010), how integrin adhesiveness is regulated on the cell surface remains controversial. Potential modes of regulation include active clustering of integrin receptors on the cell surface or release from cytoskeletal constraints and facilitated diffusion into the area of cell–cell contact (avidity regulation), and induction of increased ligand-binding affinity (affinity regulation). Activation of lymphocytes by chemokine or T-cell receptor engagement triggers LFA-1-mediated cell adhesion to endothelium or immobilized ICAM-1 within seconds or minutes, respectively (Dustin and Springer, 1989; Shamri *et al*, 2005). Paradoxically, the profound increases in binding affinity due to activating domain rearrangements measured with purified proteins *in vitro* have not been recapitulated using intact cells. Previous attempts to measure increased LFA-1 affinity for soluble ligand after inside–out activation either showed no increase (Stewart *et al*, 1996) or required the use of di- or multimeric ligands to measure avidity rather than affinity (Constantin *et al*, 2000; Bolomini-Vittori *et al*, 2009). Use of monomeric ICAM-1 in a competition assay to demonstrate LFA-1 affinity upregulation on T hybridoma cells in an early study (Lollo *et al*, 1993) has largely been discounted in view of subsequent failure to find affinity regulation (Stewart *et al*, 1996) and has never been followed up. In the absence of detectable soluble monomeric ICAM-1 binding to LFA-1, conformational changes in the α_L I domain after activation by chemokine probed by antibody (Shimaoka *et al*, 2006), exposure of activation epitopes (Shamri *et al*, 2005; Stanley *et al*, 2008; Bolomini-Vittori *et al*, 2009; Shulman *et al*, 2009), or adhesion to ICAM-1 versus ICAM-3 substrates (Tang *et al*, 2005; Li *et al*, 2007) have been used to distinguish different classes of activated LFA-1 integrins and to attribute affinity states to them. However, in the absence of actual affinity measurements, the mechanism of activation of LFA-1 has remained unclear.

Distinct mechanisms for cell surface affinity regulation have been proposed. One model suggests that talin binding to the β cytoplasmic tail disrupts a clasp with the GFFKR motif in the α subunit, allowing separation or change in orientation between the α and β subunit TM domains. This is proposed to be sufficient for activation of the extracellular integrin domains (Wegener *et al*, 2007; Ye *et al*, 2010) and predicts no difference in integrin affinity for soluble or insoluble ligands. A second model proposes that translational motion of integrins on the cell surface, that is coupled to the

actin cytoskeleton through proteins bound to the β subunit cytoplasmic domain, is associated with integrin extension and headpiece opening (Zhu *et al*, 2008). This model predicts large differences between freely diffusing and substrate-bound ligands, because resistance by ligand to translational motion increases the force that favours hybrid domain swing out and thus helps induce the high affinity state.

Here, we present the first comprehensive set of integrin monomeric affinity measurements on the surface of intact cells. A competitive radioligand-binding assay (Lollo *et al*, 1993) is used to accurately measure LFA-1 affinity over a 10 000-fold dynamic range for ligand on T lymphocytes using monovalent reagents (Figure 1E and F). The results demonstrate marked differences in the affinity state of LFA-1 when it is engaged to soluble or substrate-bound ICAM-1, and therefore support the translational motion or traction model of integrin activation over other models.

Results

Hi3-ICAM-1 binds nonactivated LFA-1 with micromolar affinity

To improve sensitivity in soluble ligand-binding assays we used Hi3-ICAM-1, an ICAM-1 mutant with five amino-acid substitutions in its binding interface that increase affinity for LFA-1 by 20-fold (Song *et al*, 2006). To measure a wide range of affinities, we used an indirect competitive radioligand-binding assay in which binding of a high affinity Fab to LFA-1 was competed off by increasing concentrations of the lower affinity Hi3-ICAM-1 ligand (Figure 1E and F). ^{125}I-labelled TS1/22 Fab, which competitively blocks ICAM-1 binding to the α_L I domain (Lu *et al*, 2004) (Figure 1E and F), bound saturably to cultured T lymphocytes with $K_{D,Fab} = 24.4 \pm 5.5$ nM and fit best to a one-site binding model (Figure 2A). An indistinguishable $K_{D,Fab} = 23.6 \pm 3.4$ nM was measured for

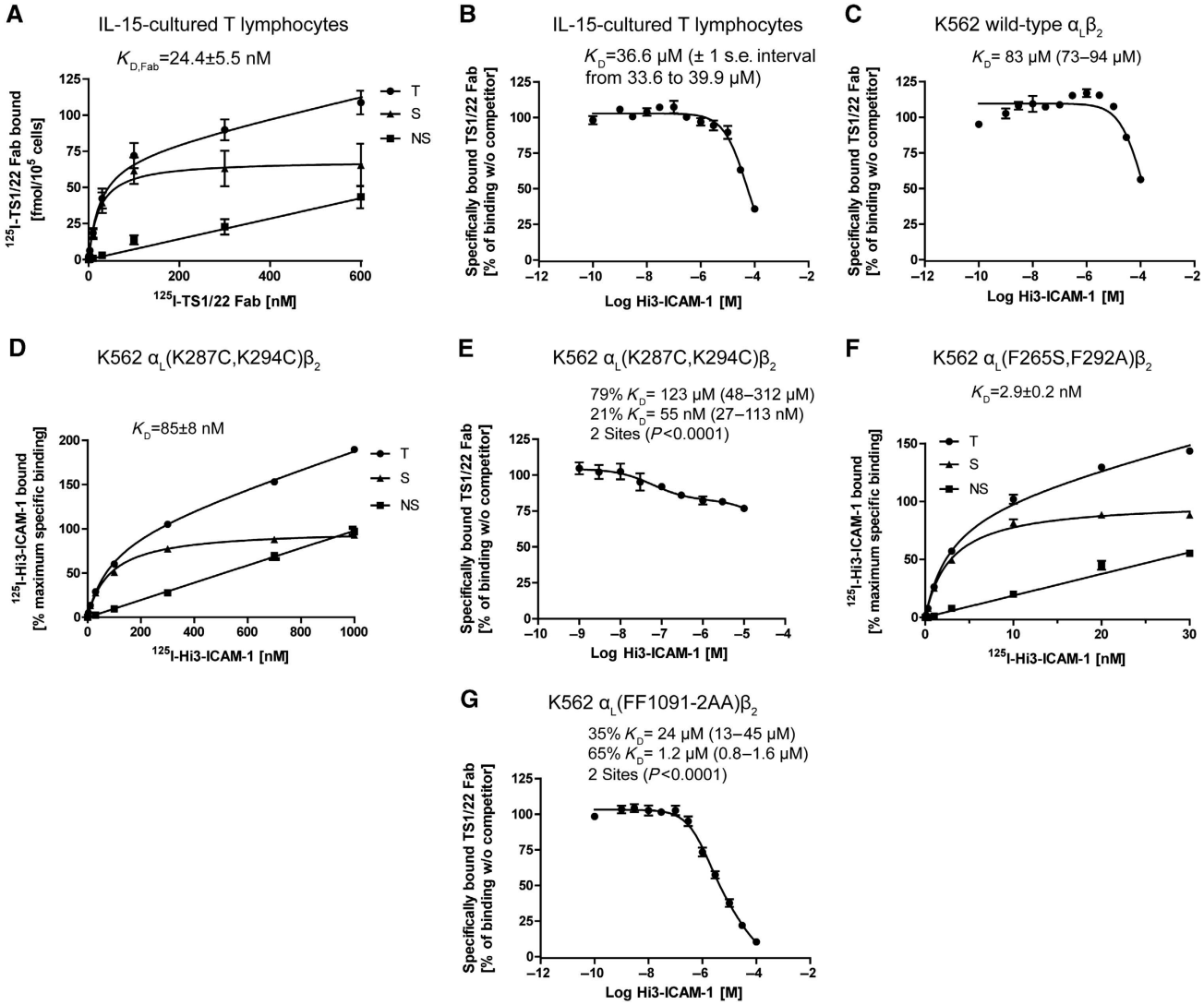

Figure 2 Soluble ligand-binding assays of LFA-1 affinity. (**A**) Saturation ^{125}I-TS1/22 Fab binding to T lymphocytes. (**B**, **C**) Competitive binding of Hi3-ICAM-1 and ^{125}I-TS1/22 Fab to cultured T lymphocytes (**B**) or K562 transfectants (**C**). (**D**, **E**) ^{125}I-Hi3-ICAM-1 saturation binding (**D**) and competitive binding of Hi3-ICAM-1 and ^{125}I-TS1/22 Fab (**E**) to high affinity (K287C, K294C) LFA-mutant K562 transfectants. (**F**) ^{125}I-Hi3-ICAM-1 saturation binding to high affinity (F265S, F292A) LFA-1-mutant K562 transfectants. (**G**) Competitive binding of Hi3-ICAM-1 and ^{125}I-TS1/22 Fab to GFFKR/GAAKR LFA-1-mutant K562 transfectants. Data are averages ± s.e. from two independent triplicate experiments. Curves are best fits to specific or total and nonspecific binding models. Specific binding (S) in (**A**, **D**, **F**) was calculated by subtracting nonspecific (NS) from total binding (T). K_D values were calculated from best-fit curves and are indicated ± s.e. (**A**, **D**, **F**) or with ± 1 s.e. intervals (**B**, **C**, **E**, **G**).

high affinity LFA-1 (Supplementary Figure S1A). Hi3-ICAM-1 competed with TS1/22 Fab for a single class of binding sites on T lymphocytes with $K_D = 36.6\,\mu M$ (33.6–39.9 μM) (Figure 2B). Hi3-ICAM-1 bound to LFA-1 on freshly isolated peripheral blood T lymphocytes with $K_D = 40.7\,\mu M$ (37.3–44.5 μM), an indistinguishable affinity from cultured T lymphocytes ($P = 0.43$) (Supplementary Figure S1B). Hi3-ICAM-1 bound with significantly lower affinity, $K_D = 83\,\mu M$ (73–94 μM, $P < 0.0001$) to LFA-1 on K562 transfectants (Figure 2C). This difference in affinity between IL-15-cultured and resting peripheral blood T lymphocytes on the one hand and K562 transfectants on the other suggests cell-type-dependent LFA-1 activation differences as previously found in adhesion assays (Hibbs *et al*, 1991; Lu and Springer, 1997; Lub *et al*, 1997).

As controls, we measured binding to two distinct $\alpha_L\beta_2$ high affinity mutants. The K287C/K294C mutation introduces a disulphide bond into the αI domain β6–α7 loop (Shimaoka *et al*, 2003b). Transfectants with this mutation are constitutively adhesive (Shimaoka *et al*, 2003b). The direct ^{125}I-Hi3-ICAM-1 binding assay shows a K_D of 85 ± 8 nM (Figure 2D). However, measuring affinity for Hi3-ICAM-1 by its ability to compete with ^{125}I-TS1/22 Fab strikingly reveals two populations of binding sites on α_L (K287C/K294C) transfectants (Figure 2E). The high affinity subpopulation of receptors of 21% binds with K_D of 55 nM (1 s.e. intervals of 27–113 nM), similar to the K_D of 85 ± 8 nM measured with direct binding. The low affinity subset of 79% binds with K_D of 123 μM, similar to the affinity of 83 μM measured with the wt LFA-1 transfectants. These results suggest that during biosynthesis, the disulphide bond conferring high affinity forms in only a subset of LFA-1 molecules, which is nonetheless sufficient for strong cell adhesiveness (Lu *et al*, 2001b). Note that saturating the low affinity sites with ^{125}I-Hi3-ICAM-1 would require 1000-fold more radiolabel than used in Figure 2D, and would result in unacceptably low signal-to-noise ratios. The ability to measure both high and low affinity sites with the ^{125}I-Fab competition assay (Figures 1F and 2E) emphasizes its power and dynamic range.

The high affinity αI domain double-mutation F265S/F292A (Jin *et al*, 2006), which renders LFA-1 constitutively adhesive (Supplementary Figure S1C), was also expressed in $\alpha_L\beta_2$ in K562 cells. Because residue Q266 in α_L forms part of the TS1/22 epitope (Lu *et al*, 2004) and the neighbouring F265S mutation completely abolishes TS1/22 binding (data not shown), we directly measured ^{125}I-Hi3-ICAM-1 binding with $K_D = 2.9 \pm 0.2$ nM (Figure 2F). The higher affinity of the F265S/F292A mutation compared with K287C/K294C is in agreement with the comparably higher affinity of F265S/F292G than K287C/K294C mutant in isolated α_L I domains measured with surface plasmon resonance (Jin *et al*, 2006).

Mutating the highly conserved GFFKR sequence at the TM domain/cytoplasmic domain boundary of α_L to GAAKR disrupts α_L and β_2 cytoplasmic domain association (Kim *et al*, 2003) and induces constitutive activation of LFA-1 and exposure of activation epitopes (Lu and Springer, 1997). Disrupting this intracellular clasp by mutation is commonly used to mimic integrin inside–out activation. The GFFKR/GAAKR mutation resulted in two distinct LFA-1 subpopulations and increased affinity to $K_D = 24\,\mu M$ (13–45 μM) in 35% of the receptors and to $K_D = 1.2\,\mu M$ (0.8–1.6 μM) in 65% of LFA-1 (Figure 2G), compared with $K_D = 83\,\mu M$ for wt LFA-1. Below, we operationally refer to an increase in affinity to the 20–30 μM level as priming, to the 1–20 μM level as intermediate affinity, and to the lower nanomolar range as high affinity.

Physiological activation of lymphocytes induces integrin priming

Activation of T lymphocytes is triggered by T-cell receptor (TCR) stimulation or by chemokines and can be mimicked by the protein kinase C activator phorbol-12-myristate-13-acetate (PMA). Activation of cultured T lymphocytes by PMA, chemokine stromal cell-derived factor (SDF)-1α, or by crosslinking TCRs induced adhesiveness to immobilized ICAM-1 (Figure 3A–C). The integrin activator Mn^{2+} (Dransfield *et al*, 1992) served as a positive control (Figure 3D). All three T lymphocyte activators induced primed LFA-1 that bound Hi3-ICAM-1 significantly better than control with K_D values between 25 and 27 μM, as opposed to K_D values between 35 and 37 μM in control cells (Figure 3E–G). Constraining maximal binding in Figure 3E–G to 100% did not alter this conclusion, and differences between affinities remained significant (Supplementary Figure S2A–C). Freshly isolated peripheral T lymphocytes showed a similar SDF-stimulated increase in affinity to $K_D = 24.7\,\mu M$ (22.3–27.4 μM) (Supplementary Figure S1D), not distinct from SDF-1α-stimulated cultured T lymphocytes ($P = 0.77$). Mn^{2+} induced intermediate affinity LFA-1 with $K_D = 462$ nM (425–503 nM) (Figure 3H). Induction of lymphocyte adhesion and the primed or intermediate affinity state of LFA-1 were paralleled by increased exposure of the m24 and KIM127 activation epitopes (Figure 3I), in agreement with previous reports (Lu *et al*, 2001a). The m24 antibody binds to activated β_2 I domains (Lu *et al*, 2001c; Chen *et al*, 2010) and the KIM127 antibody recognizes an epitope on β_2 I-EGF2 domain that is exposed upon integrin activation (Lu *et al*, 2001a) (Figure 1C). The highest activation epitope exposure was observed after activation by Mn^{2+} (Figure 4I), in agreement with its strong affinity-increasing effect.

The open integrin headpiece is required for adhesion and high affinity for soluble ligand

The absence of high affinity for soluble ligand after inside–out activation of LFA-1 suggested either that adhesion did not require high affinity, or cellular pathways that increased affinity for immobilized but not soluble ligands. To bypass the requirement for adhesion-dependent modulation of affinity, we examined function-perturbing antibodies. Several well-characterized antibodies to LFA-1 are available that stabilize and/or induce activating LFA-1 conformations. Activating CBR LFA-1/2 binds to the I-EGF3 domain on β_2 and induces an extended conformation (Petruzzelli *et al*, 1995; Lu *et al*, 2001a; Nishida *et al*, 2006). MEM148 recognizes an activation epitope on the β_2 hybrid domain and stabilizes hybrid domain swing out (Drbal *et al*, 2001; Tang *et al*, 2005; Chen *et al*, 2010) (Figure 1C). To exclude potential LFA-1 crosslinking on the cell surface by dimeric IgG, we used Fab fragments throughout.

We measured lymphocyte adhesion and LFA-1 affinity induced by CBR LFA-1/2, KIM127, and MEM148 alone or in various combinations with each other. The activating Fab induced lymphocyte adhesion to ICAM-1 substrates (Figure 4A). Binding of CBR LFA-1/2 induced exposure

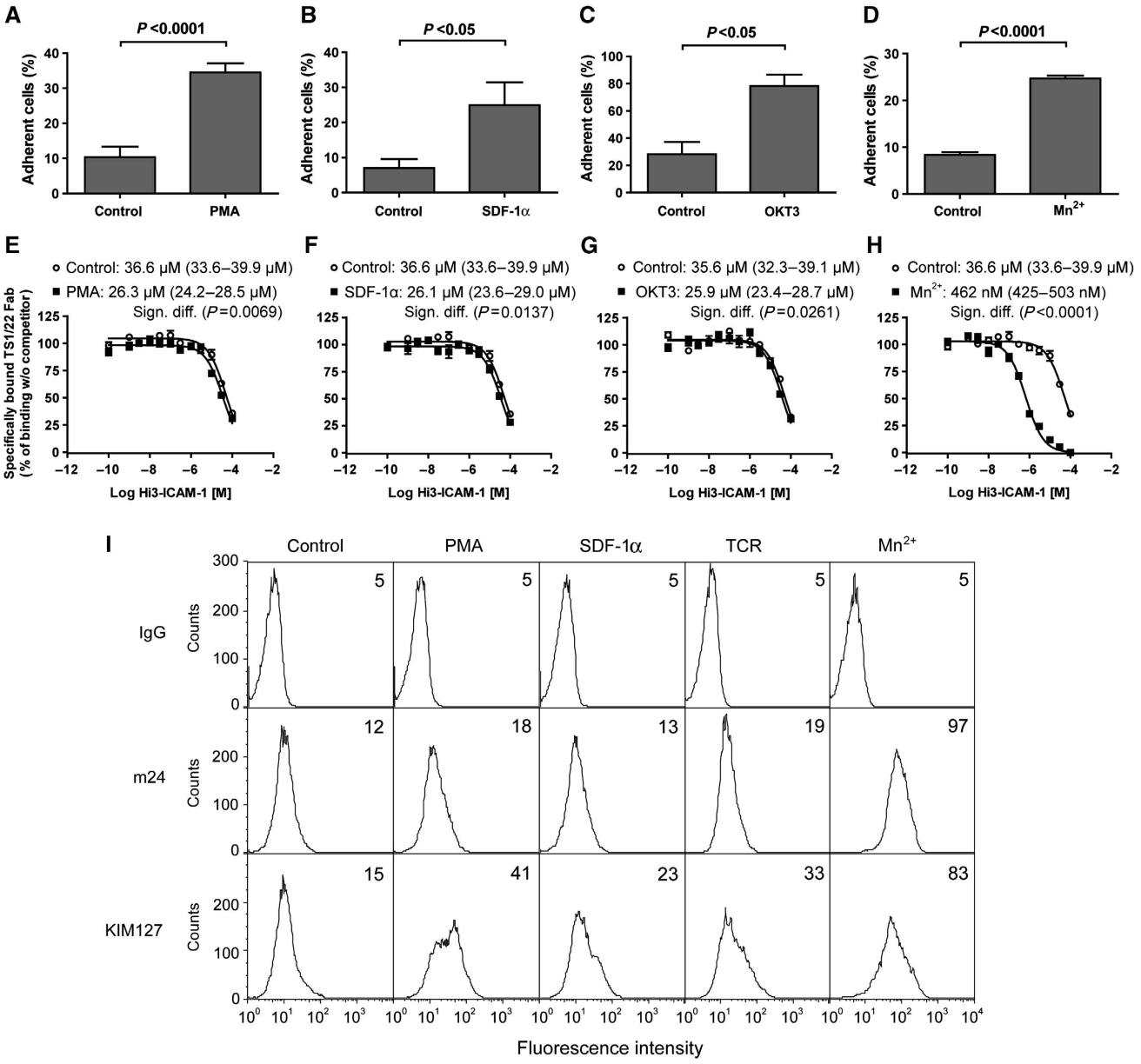

Figure 3 Inside–out activation of LFA-1 on T lymphocytes induces integrin priming. Lymphocyte adhesion to ICAM-1 substrates (**A**–**D**) and Hi3-ICAM-1 competition binding (**E**–**H**) after activation by PMA (**A**, **E**), SDF-1α (**B**, **F**), crosslinking TCR with OKT3 plus anti-IgG_{2a} (**C**, **G**), or Mn^{2+} activation (**D**, **H**). Control was medium (**A**, **B**, **D**–**F**, **H**) or mouse IgG_{2a} plus anti-IgG_{2a} antibody (**C**, **G**). Adhesion results are averages ± s.e. ($n = 3$–9) and *P* values are from two-tailed unpaired *t*-tests. Activation was for 30 min (**A**, **D**), 2 min (**B**), or 10 min (**C**). Hi3-ICAM-1 binding data are averages ± s.e. ($n = 2$, in triplicates). Control data for (**E**, **F**, **H**) are from Figure 2B. Affinity values were calculated from best-fit curves and indicated with ± s.e. intervals in parentheses. Affinities were compared with control by F-tests. (**I**) KIM127 and m24 activation epitope exposure after cell activation. Numbers indicated are mean fluorescence intensities and are representative for two independent experiments.

of activation epitopes KIM127 and m24 (Figure 4B). Intermediate LFA-1 affinity for soluble ligand with $K_D = 9.2\,\mu M$ (8.4–10.2 μM) or $K_D = 17.9\,\mu M$ (16.6–19.4 μM) was observed after activation with CBR LFA-1/2 or MEM148, respectively (Figure 4C and D). The absence of high affinity LFA-1 after activation by MEM148 is consistent with the previous observation that MEM148 requires LFA-1 activation for full reactivity (Tang *et al*, 2005). KIM127, the strongest adhesion-promoting Fab, induced 72% intermediate affinity LFA-1 with $K_D = 3.1\,\mu M$ (2.6–3.6 μM) and 28% high affinity LFA-1 with $K_D = 13$ nM (8–22 nM) (Figure 4E). The population of cell surface molecules with high affinity LFA-1 was further increased to 73% by adding both CBR LFA-1/2 and KIM127 (Figure 4F), in agreement with a strong induction of cell adhesion by this combination (Figure 4A). Induction of high affinity LFA-1 by this antibody combination is remarkable, since both epitopes are located on the integrin leg, suggesting that strong leg activation either directly triggers conformational rearrangements in the integrin headpiece or communicates signals to the cytoplasm that activate high affinity for ligand. Even CBR LFA-1/2 Fab alone partially induced headpiece opening as shown with m24 epitope expression (Figure 4B), which reports βI domain opening (Chen *et al*, 2010).

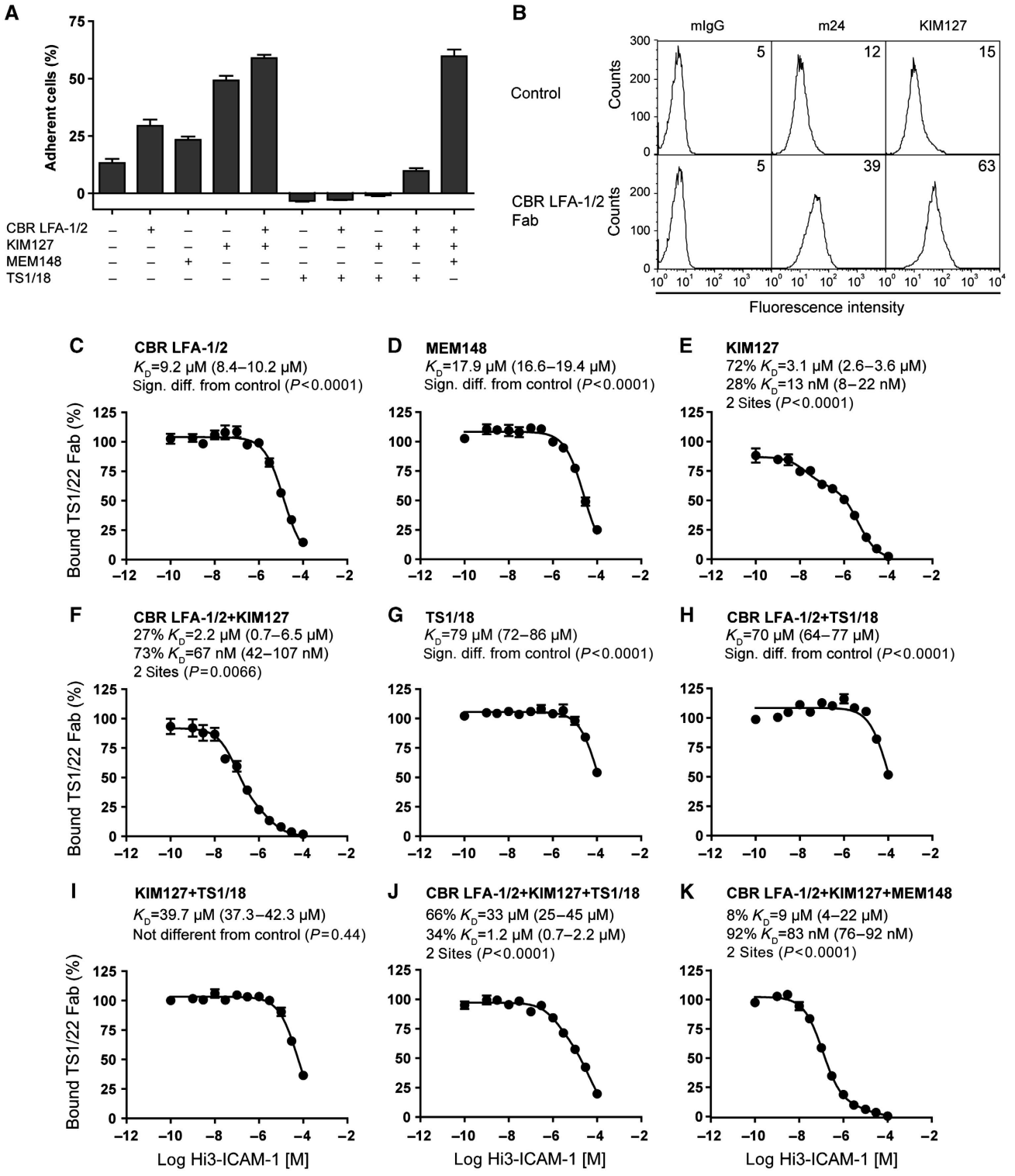

Figure 4 The open LFA-1 headpiece is required for adhesion and high affinity for soluble ligand. (**A**) Lymphocyte adhesion to ICAM-1 substrate after activation by Fab. Averages ± s.e. (n = 3–13). (**B**) Activation epitope exposure after CBR LFA-1/2 Fab activation of LFA-1. Mean fluorescence intensities are indicated and representative of two independent experiments. (**C**–**K**) Competition binding of Hi3-ICAM-1 after LFA-1 activation by Fab. Results are averages ± s.e. from two independent triplicate experiments. Curves are best fits. Calculated K_D values with s.e. interval are in parentheses. Affinities in one-site binding models were compared with control (Figure 2B) by F-test and P values are shown. If data fit significantly better to a two-site binding model (F-test), P values and results for both receptor populations are shown.

We further examined the role of headpiece opening (Figure 1B and C) in LFA-1 affinity. To test if the open headpiece conformation was important in the high affinity state, we used TS1/18. This inhibitory antibody binds to the β_2 I domain, is allosteric as shown by ability to block ligand binding by wt LFA-1 but not LFA-1 with a locked open αI domain (Lu *et al*, 2001c), and has been demonstrated by EM to induce the closed headpiece (Chen *et al*, 2010). When

added to nonactivated lymphocytes or lymphocytes activated by CBR LFA-1/2 or KIM127, TS1/18 completely blocked adhesion to ICAM-1 substrate (Figure 4A). In lymphocytes activated by the combination of CBR LFA-1/2 and KIM127, TS1/18 reduced adhesion below the levels of nonactivated control cells (Figure 4A). Interestingly, stabilizing the closed headpiece in nonactivated cells by TS1/18 significantly lowered LFA-1 affinity for ligand to $K_D = 79\,\mu M$ (72–86 μM) (Figure 4G), a level similar to that in K562 transfectants (Figure 2C). This is below the affinity on T lymphocytes (Figure 4G; $P < 0.0001$), suggesting that T lymphocytes, in contrast to K562 transfectants, express LFA-1 with a partially active headpiece. A similar reduction to $K_D = 70\,\mu M$ (64–77 μM) was observed when adding TS1/18 to lymphocytes activated by CBR LFA-1/2 (Figure 4H). Induction of high affinity LFA-1 by KIM127 or CBR LFA-1/2 + KIM127 was completely blocked by TS1/18 (Figure 4I and J), and the resulting affinity of $K_D = 39.7\,\mu M$ (37.3–42.3 μM) in KIM127-activated lymphocytes treated with TS1/18 was indistinguishable from basal affinity (Figure 4I; $P = 0.44$). In the presence of CBR LFA-1/2 and KIM127, TS1/18 did not completely abolish the primed state (Figure 4J) and some adhesiveness remained (Figure 4A). We attribute this to incomplete saturation by TS1/18 in the face of competing allosteric effects of the other antibodies, as confirmed by titrations in cell adhesion assays (Supplementary Figure S3).

In contrast to TS1/18, which stabilizes the closed headpiece, addition to CBR LFA-1/2 + KIM127 of MEM148, which stabilizes the open headpiece, increased the high affinity population size from 73 to 92% (Figure 4K), the largest high affinity LFA-1 population of all Fab combinations tested. When using ^{125}I-Hi3-ICAM-1 to directly measure the affinity for wt LFA-1 receptors stabilized in a high affinity state, we found a $K_D = 36.9 \pm 3.0\,nM$ (Supplementary Figure S4), in good agreement with the data from competition experiments (Figure 4K). These results show for the first time that LFA-1 on the T lymphocyte surface can adopt an open headpiece conformation that binds monomeric ligand with nanomolar affinity. The adhesion assay results further show that the open headpiece is required for cell adhesion.

Communication between the open headpiece and the α_L I domain is required for adhesion and high affinity for soluble ligand

In contrast to integrins that lack αI domains, the presence of the ligand-binding α_L I domain in LFA-1 adds another level of integrin regulation. Ligand binding to LFA-1 appears to be activated by interaction of α_L Glu-310, which follows the α_L I domain α7-helix, with the β_2 MIDAS (Figure 1C) (Huth *et al*, 2000; Alonso *et al*, 2002; Yang *et al*, 2004). We used three well-characterized allosteric LFA-1 inhibitors to study α_L I domain activation by interaction with the β_2 subunit. BIRT377 is an αI allosteric inhibitor that binds under the C-terminal α7 helix of the α_L I domain (Figure 1A), thereby preventing the downward movement of this helix and stabilizing the α_L I domain in an inactive, closed conformation (Kallen *et al*, 1999; Last-Barney *et al*, 2001; Weitz-Schmidt *et al*, 2001). XVA143 and compound #4 are members of a second class of LFA-1 antagonists, the α/β I allosteric inhibitors, that are believed to bind to the βI domain MIDAS and block αI activation by preventing binding of the intrinsic β_2 MIDAS ligand α_L-E310 (Shimaoka and Springer, 2003) (Figure 1D).

BIRT377 did not induce m24 and KIM127 epitope expression on T lymphocytes (Figure 5A). In contrast, XVA143 and compound #4 induced β_2 leg extension and βI domain opening, as demonstrated by KIM127 and m24 epitope exposure, respectively (Figure 5A) (Shimaoka *et al*, 2003a; Salas *et al*, 2004; Yang *et al*, 2006). XVA143 and compound #4 induced stronger exposure of these epitopes than Mn^{2+} (compare Figures 3I and 5A).

BIRT377 inhibited PMA-induced lymphocyte adhesion to ICAM-1 (Figure 5C) and lowered Hi3-ICAM-1 binding affinity to $K_D = 169\,\mu M$ (140–203 μM) (Figure 5B). This value is significantly lower than in control cells ($P < 0.0001$), again showing that LFA-1 on T lymphocytes has basal activity. A small amount of LFA-1-independent adhesiveness, which was revealed by the LFA-1-specific inhibitor BIRT377, was inhibited by the anti-Mac-1 ($\alpha_M\beta_2$) antibody M1/70 (Figure 5C), in agreement with Mac-1 expression by IL-15-cultured T lymphocytes. In SKW3 T lymphoblastoid cells, which express LFA-1 but no Mac-1, PMA-induced cell adhesion to ICAM-1 was completely blocked by all three tested compounds (Figure 5C).

While the allosteric antagonist XVA143 did not alter LFA-1 affinity for ligand, compound #4 induced intermediate affinity similar to CBR LFA-1/2 (Figure 5B). This agrees with a previous report that compound #4 but not XVA143 increases binding of multimeric ICAM-1 to cell surface LFA-1 (Yang *et al*, 2006). The induction of intermediate affinity LFA-1 by compound #4 is in sharp contrast with its ability to completely block phorbol ester-induced adhesion of both primary T lymphocytes and SKW3 cells to ICAM-1 (Figure 5C). These data suggest that intermediate affinity LFA-1 is not sufficient for adhesion to ICAM-1.

XVA143 induces hybrid domain swing out (Nishida *et al*, 2006), but by binding to the βI MIDAS, blocks communication of headpiece opening to αI domain activation. We further confirmed the mode of inhibition of LFA-1 affinity maturation by testing the hypothesis that XVA143 would also prevent activation by Fab that bind distal to this interface. Since the MEM148 Fab binds to the β_2 hybrid domain to stabilize the open headpiece conformation, and CBR LFA-1/2 and KIM127 bind to the β_2 leg, their effects on ligand binding to the α_L I domain should require communication through the interface between the βI and αI domains. Indeed, whereas combination of the three Fab induced a substantial population of high affinity sites, this was completely blocked by XVA143 (Figure 5D). Furthermore, XVA143 completely blocked adhesiveness stimulated by the three Fab (Figure 5E).

The importance of α/β I communication was further tested by mutating α_L residue Glu-310, the putative intrinsic ligand for the β_2 MIDAS. The affinity of the α_L-E310A mutant LFA-1 of 561 μM (391–806 μM) was significantly lower than wt LFA-1 of 83 μM in K562 transfectants (Figure 5F). The lower affinity of the E310A mutant than wt LFA-1 in K562 transfectants suggests a low level of coupling between the αI and βI domains through E310 in wt, which makes affinity higher than it would otherwise be. Importantly, the CBR LFA-1/2, KIM127, and MEM148 Fab combination could not stimulate the high affinity state of E310A, although a slight increase in affinity to 281 μM occurred (Figure 5F). This may suggest a low level of coupling between the αI and βI domains in the absence of Glu-310. In summary, adhesion and high affinity of LFA-1 each require communication between the open headpiece and the αI domain.

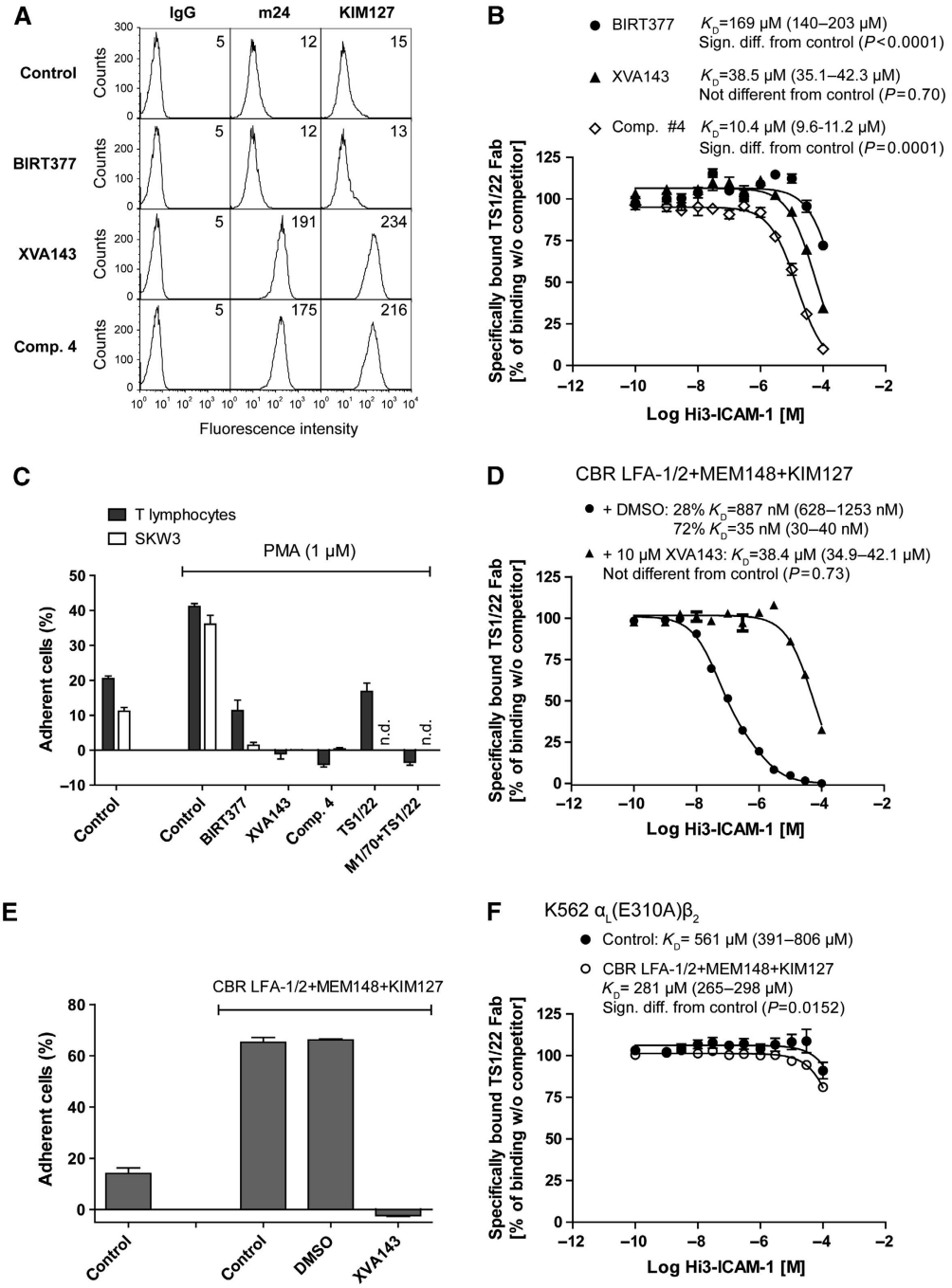

Figure 5 Communication between the open headpiece and the α_L I domain is required for adhesion and high affinity for soluble ligand. (**A**) m24 and KIM127 activation epitope exposure. Indicated mean fluorescence intensities are representative of two independent experiments. (**B**, **D**, **F**) Competition binding of Hi3-ICAM-1 to T lymphocytes (**B**, **D**) and K562 transfectants (**F**). Data are average ± s.e. from two independent triplicate experiments. Curves are best fits and affinities are given with s.e. intervals in parentheses. Affinities were compared to control (Figure 2B) (**B**, **D**) or nonactivated K562 transfectants (**F**) by F-tests and *P* values are shown. (**C**, **E**) T lymphocyte (**C**, **E**) and SKW3 cell (**C**) adhesion to ICAM-1 substrate. n.d., not determined. Results are averages ± s.e. of triplicates.

Transition of primed or intermediate affinity LFA-1 to the adhesive high affinity state is energy dependent

Our results demonstrate that primed LFA-1 requires headpiece opening and αI domain activation to acquire high affinity and adhesiveness and suggest that the signal required for these conformational changes is provided by engaging immobilized ligand. To test this hypothesis, intracellular energy stores in T lymphocytes were depleted by incubation with sodium azide and 2-deoxy-D-glucose. Energy depletion abolished basal cell adhesion to ICAM-1 without altering basal soluble ligand-binding affinity (Figure 6A and B). Also, adhesion induced by CBR LFA-1/2 or MEM148 Fab was abolished in the absence of intracellular energy (Figure 6A). Each Fab induces an intermediate affinity state in LFA-1 (Figure 4C and D), and this once again demonstrates that intermediate affinity is not sufficient to support cell adhesion. As expected, the adhesion-inducing activity of PMA, which activates protein kinase C, was blocked by

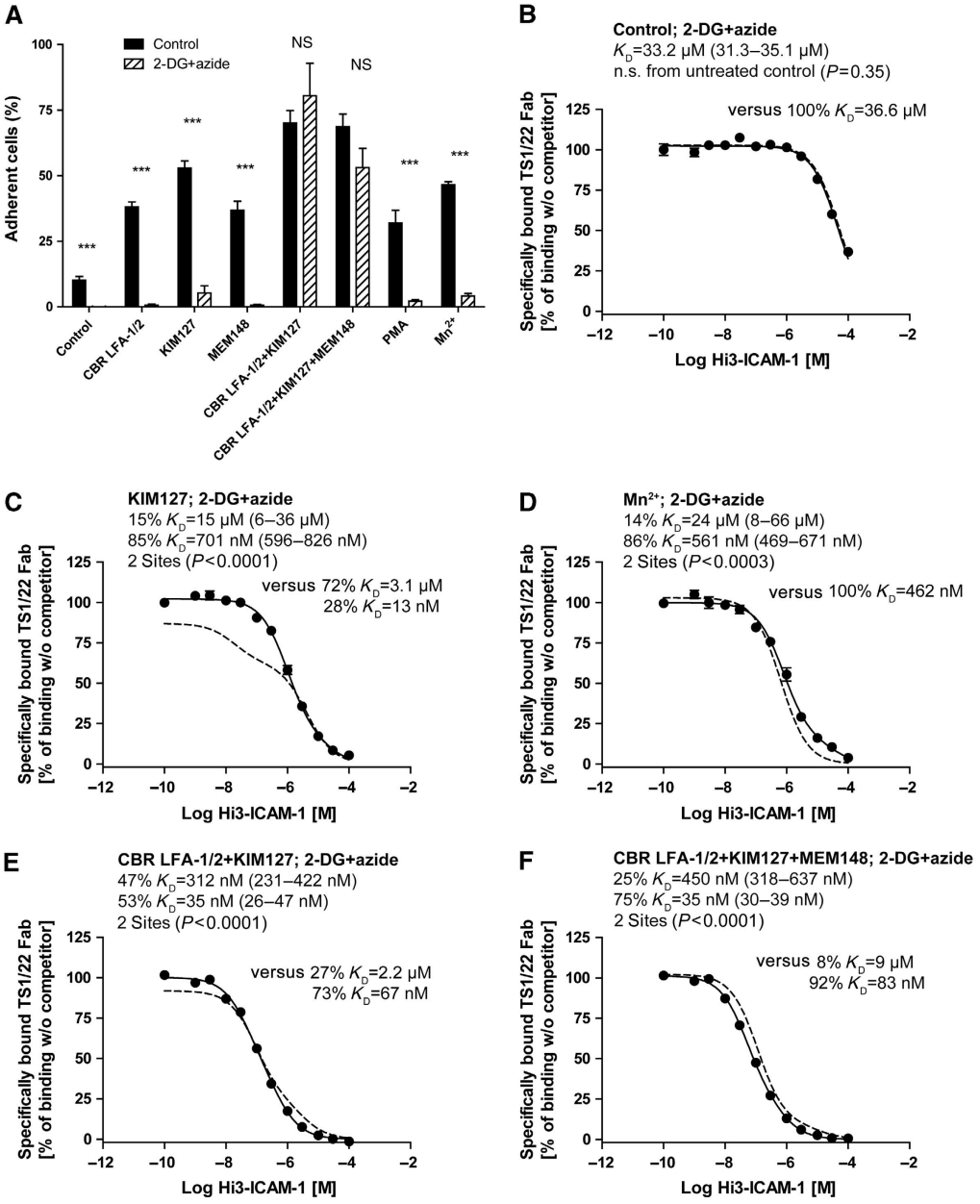

Figure 6 Conversion from primed or intermediate affinity to adhesive high affinity LFA-1 requires cellular energy. (**A**) T lymphocyte adhesion to ICAM-1 after pretreatment of cells with 2-deoxy-glucose (2-DG) and sodium azide. Shown are averages ± s.e. ($n = 8$–9). Mean values were compared by unpaired two-tailed *t*-tests with Welch's correction (***$P < 0.001$; NS, not significant). (**B**–**F**) Competition binding of Hi3-ICAM-1 to T lymphocytes pretreated with 2-DG and azide and stimulated with various activators. Data are shown as average ± s.e. from two independent triplicate experiments. Solid lines are best fits to data and affinities are given with s.e. intervals in parentheses. If data fit significantly better to a two-site binding model (F-test), *P* values and results for both receptor populations are shown. For comparison, data from Figures 2–4 on cells without pretreatment are shown as dashed lines, with affinities and receptor populations in those samples shown after 'versus'.

energy depletion (Figure 6A). Most strikingly, the strong adhesion-inducing activity of KIM127 Fab required energy (Figure 6A), and the 28% high affinity LFA-1 population observed after activation by KIM127 (Figure 4E) was absent after energy depletion (Figure 6C). This suggests that binding of KIM127 induces inside–out signalling, resulting in a high affinity LFA-1 population, and explains the strong adhesion-inducing activity of KIM127.

Further observations supported the requirement of energy for affinity maturation and adhesiveness. There was little effect of energy depletion on the intermediate affinity of LFA-1 in the presence of Mn^{2+} (Figure 6D). However, adhesiveness in Mn^{2+} was abolished by energy depletion. This suggests that the affinity level induced by manganese and the incompletely opened integrin headpiece requires intracellular energy for conversion into the high affinity state required for cell adhesion. The combination of activating CBR LFA-1/2 and KIM127 with or without MEM148 stabilized the majority of LFA-1 integrins in a high affinity conformation (Figure 4F and K). These high affinity receptor populations were mostly resistant to energy depletion (Figure 6E and F). Consistent with this observation, both Fab combinations conferred

integrin adhesiveness that was independent of intracellular energy (Figure 6A). Taken together, these data provide strong evidence that LFA-1 with a partially opened headpiece (primed or intermediate affinity) requires an energy-dependent intracellular process for complete headpiece opening and transitioning to a fully adhesive conformation with high affinity for ligand.

Discussion

Many labs including our own have reported on affinity regulation of LFA-1 on intact cells. However, these studies measured changes in adhesiveness to ligands on substrates (Dustin and Springer, 1989; Tang *et al*, 2008), binding of bivalent ICAM-1 or higher valency ICAM-1 multimers (Stewart *et al*, 1996; Ganpule *et al*, 1997; Constantin *et al*, 2000; Kim *et al*, 2004; Bolomini-Vittori *et al*, 2009), or binding of activation-dependent antibodies (Shamri *et al*, 2005; Shimaoka *et al*, 2006; Stanley *et al*, 2008; Bolomini-Vittori *et al*, 2009; Feigelson *et al*, 2010); furthermore, changes in binding rather than actual affinities have been reported. Generally, no binding of a dimeric or multimeric ligand has been found in the resting state. Reports have differed on the activated state. Some labs have found multimeric ligand binding and/or activation-dependent antibody binding after stimulation with Mn^{2+} or other agents, and no detectable binding after physiologic stimulation (Stewart *et al*, 1996; Ganpule *et al*, 1997); others have found detectable binding after PMA or chemokine stimulation (Constantin *et al*, 2000; Kim *et al*, 2004; Shimaoka *et al*, 2006; Bolomini-Vittori *et al*, 2009; Shulman *et al*, 2009). Early on, the results were interpreted as ruling out affinity regulation of LFA-1, and supporting alternative models such as clustering in the membrane and/or increased diffusiveness, and regulation of adhesiveness by avidity rather than affinity regulation (Kucik *et al*, 1996; Stewart *et al*, 1996; van Kooyk *et al*, 1999). More recently, post-ligand binding events have been invoked (Ganpule *et al*, 1997; Shamri *et al*, 2005; Feigelson *et al*, 2010), based in part on the observation that cell surface LFA-1 that appears to be in contact with ICAM-1 on the substrate stains with activation-dependent antibodies (Stanley *et al*, 2008; Feigelson *et al*, 2010). However, none of these papers reported affinity measurements for LFA-1 in the resting or active state, and thus considerable uncertainty has remained about whether or how affinity regulation contributes to adhesiveness. Only a single report, never followed up, demonstrated a modest increase in affinity for ICAM-1 after stimulation of mouse T hybridoma cells by PMA (Lollo *et al*, 1993).

We present the first comprehensive measurements of LFA-1 affinities on the cell surface and the first demonstration that a high affinity state of LFA-1 is required for cell adhesion. Previous comparison of wt ICAM-1 and Hi3-ICAM-1 affinities for both intermediate and high affinity mutant I domains by surface plasmon resonance measurements supports multiplying the K_D values obtained here with Hi3-ICAM-1 by 20-fold to compute wt ICAM-1 affinities for cell surface LFA-1 (Song *et al*, 2006). In the following discussion, we use this conversion factor to report estimates of wt ICAM-1 K_D values. We demonstrate that wt cell surface LFA-1 is capable of exhibiting a wide range of affinities from a K_D value of 1.7 mM on the surface of K562 transfectants to 260 nM on lymphocytes in the presence of KIM127 Fab, a dynamic range of 6000-fold. When the α_L E310A mutant is included (11 mM), the dynamic range we have measured on cell surfaces is 40 000-fold, comparable to the previous dynamic range of mutant α_L I domains crystallized in closed, intermediate, and open conformations (Shimaoka *et al*, 2003b; Jin *et al*, 2006). Thus, our results suggest that the full range of αI domain conformational states visualized in crystals is accessible on cell surfaces. It is however important to note that the wide range of affinities measured here suggests that we are measuring values not for fixed conformational states on the cell surface, but for LFA-1 molecules in dynamic equilibrium between different conformational states. Furthermore, in many conditions, we obtained evidence for at least two distinct subpopulations of LFA-1 molecules on the cell surface with distinct affinities.

To simplify discussion, we refer to low, basal, primed, intermediate, and high affinity states. One of our important observations is that LFA-1 on primary and cultured T lymphocytes is in a basal, rather than a low affinity state. This resolves a major conundrum of how LFA-1 could mediate migration of unstimulated lymphocytes on ICAM-1 substrates, while also providing a 'stop signal' when foreign antigen or chemokine is encountered (Dustin *et al*, 1997). This has been seen *in vitro* on ICAM-1 substrates and endothelial cells, and *in vivo* in lymph nodes, when lymphocytes engage in many brief adhesive encounters with non-antigen-bearing cells, while engaging in prolonged encounters when specific antigen is recognized (Dustin *et al*, 1997; Mempel *et al*, 2004; Shamri *et al*, 2005). We find that the K_D for ICAM-1 of LFA-1 on K562 transfectants is significantly lower than on resting lymphocytes, in agreement with previous observations on cell-type-dependent differences in LFA-1 adhesiveness (Hibbs *et al*, 1991; Lu and Springer, 1997; Lub *et al*, 1997). Furthermore, a five-fold decrease in affinity of LFA-1 on lymphocytes occurred when a drug was added that binds under the α_L α7-helix and stabilizes the closed αI domain conformation. Mutation of Glu-310 to Ala decreases LFA-1 adhesiveness and basal binding of KIM127 antibody to the β_2 leg (Huth *et al*, 2000; Salas *et al*, 2004). We found a seven-fold reduction in basal affinity of LFA-1 on K562 transfectants in the α_L E310A mutant. These findings demonstrate that even in K562 transfectants, LFA-1 has some basal ICAM-1-binding activity. On T lymphocytes, TS1/18 Fab to the β_2 I domain, which binds to bent-closed and extended-closed but not extended-open β_2 integrins (Chen *et al*, 2010), reduced affinity significantly below basal levels, suggesting that the time-averaged affinity in the basal state includes a contribution from the extended-open conformation of LFA-1. The α_L GFFKR/GAAKR mutation increases affinity 70-fold in K562 transfectants. Collectively, these findings demonstrate cell-specific differences in basal LFA-1 affinity for ICAM-1 that are dependent on conformational coupling of the α_L I domain through multiple integrin domain–domain interfaces all the way to the membrane-cytoplasm boundary at the GFFKR motif (Lu and Springer, 1997; Lau *et al*, 2009; Zhu *et al*, 2009). High basal affinity appears to be a specialization of LFA-1, because it exhibits greater constitutive exposure of activation epitopes than $\alpha_M\beta_2$ and $\alpha_x\beta_2$ (Lu *et al*, 2001a), and greater extension than $\alpha_x\beta_2$ in clasped ectodomain constructs (Nishida *et al*, 2006).

We demonstrated clear increases in LFA-1 affinity upon stimulation with TCR crosslinking, chemokine addition, and

activation of protein kinase C by PMA. Although these increases were modest, they were reproducible in independent experiments and statistically significant in each case. Monomeric affinity of individual LFA-1 molecules was increased, presumably through altered interactions with cytoplasmic effectors in stimulated cells. Furthermore, the increased affinity for soluble ligand was associated with increased cellular adhesiveness. However, studies with allosteric α/β antagonists demonstrated that these modest affinity increases were not sufficient for increased adhesiveness. Indeed, XVA143 reduced cell adhesiveness below basal levels, but had no significant effect on affinity. More remarkably, compound #4 increased monomeric affinity to levels higher than physiologic activators, yet completely abolished basal adhesion. Thus, the modest affinity increase seen in priming is not sufficient for adhesiveness. Allosteric α/β antagonists stabilize the open integrin headpiece but block activation of the α_L I domain by the β_2 MIDAS (Shimaoka *et al*, 2003a). These results therefore demonstrate that strong activation of the α_L I domain, involving binding of α_L Glu-310 to the β_2 MIDAS, is required for LFA-1 adhesiveness.

The importance of conformational changes in regulation of monomeric LFA-1 affinity and adhesiveness was further explored with Fab. Fab that favoured integrin extension or headpiece opening, as shown in EM studies with the sister integrin $\alpha_x\beta_2$ (Nishida *et al*, 2006; Chen *et al*, 2010), each individually increased adhesiveness and monomeric affinity for ligand. The similar effects of antibodies that promote extension and opening demonstrate linkage in cell surface LFA-1 between equilibria for integrin extension and headpiece opening. Experiments with allosteric Fab that induced or inhibited headpiece opening demonstrated that the fully open headpiece conformation of LFA-1 in which there is swing out of the hybrid domain at its junction with the β I domain is absolutely required for cell adhesion and high affinity binding. This state has an affinity similar to that previously measured for an αI domain mutationally stabilized in the open conformation (Shimaoka *et al*, 2003b; Jin *et al*, 2006; Song *et al*, 2006), demonstrating for the first time that wt LFA-1 can be stabilized in a high affinity conformation on the lymphocyte surface. Extended LFA-1 with a closed headpiece did not have increased affinity and did not mediate adhesion. XVA143 and the α_L E310A mutation completely blocked induction of the high affinity state by CBR LFA-1/2 + KIM127 + MEM148 Fab, demonstrating the importance of the αI/βI interface.

Our results demonstrate that the open headpiece conformation of LFA-1 is required for cell adhesion and has high affinity for ICAM-1. However, physiologic activators of adhesion induced quite modest increases in affinity for soluble ligand. The induction of the high affinity state in cell adhesion to immobilized ICAM-1 but not in binding to soluble ICAM-1 demonstrates that cells can sense the difference between soluble and immobilized integrin ligands (Ganpule *et al*, 1997). In other words, binding to immobilized ligands must induce unique 'post-ligand binding events'.

The effects of KIM127 Fab, α/β I allosteric antagonists, and α_L E310A mutation demonstrate that the αI/βI interface is required for these post-ligand binding events. The results with KIM127 were particularly telling. KIM127 induced ~30% of cell surface molecules to populate the high affinity state. Remarkably, this high affinity LFA-1 population but not an intermediate affinity population of receptors induced by KIM127 were sensitive to energy depletion. These findings suggest that binding of KIM127 is sensed within the cell and triggers signals that induce headpiece opening. Among four activating mAb characterized in EM on $\alpha_x\beta_2$ and tested for effect on LFA-1 affinity, including CBR LFA-1/2, MEM148, and m24 (data not shown), KIM127 is unique. Perhaps, the distinctive feature is that KIM127, in contrast to CBR LFA-1/2, binds in between the α and β legs (Nishida *et al*, 2006). We speculate that KIM127, more than the other tested Fab, favours separation of the α and β subunit TM and cytoplasmic domains, and that this triggers post-ligand binding events that induce hybrid domain swing out. On the other hand, adding CBR LFA-1/2 or additionally MEM148 Fab was found to be sufficient to yield high affinity LFA-1 in the absence of cellular energy, and cell adhesion. Chilling cells on ice had a similar effect to energy depletion—KIM127 alone did not induce high affinity at 0 °C, while the KIM127 + CBR LFA-1/2 combination did (Supplementary Figure S5). Thus, measuring LFA-1 affinity and adhesiveness in the presence of different Fab and in the presence and absence of energy demonstrated the absolute dependence of cell adhesion on the high affinity state. Interestingly, the intermediate affinity stimulated by Mn^{2+} was not sufficient for cell adhesion in the absence of energy. Thus, Mn^{2+}, as well as inside–out signalling, requires post-ligand binding events for maturation of LFA-1 into a high affinity state that is competent for cell adhesion.

While post-ligand binding events have previously been suspected as important for regulating adhesiveness, their nature has been unclear. Our results for the first time demonstrate that the key event is conversion of LFA-1 itself to the high affinity state.

Our results discriminate between models of integrin activation that either do, or do not, differentially affect affinity for soluble and insoluble ligands (Figure 7). Although we have not directly measured affinities for ligands on substrates, the demonstration with Fab that the open headpiece conformation of LFA-1 is required for cell adhesion and that this conformation on lymphocytes has high affinity for monomeric ICAM-1, demonstrates that high affinity is required for cell adhesion, a major advance in the field. Among currently proposed models for integrin activation, the translational motion or traction force model (Zhu *et al*, 2008) successfully predicts the key difference observed here in integrin affinity for ligands in solution phase and on substrates (Figure 7).

The translational motion or traction model (Figure 7C) shares with other models (Figure 7B) the importance of binding to the integrin β subunit cytoplasmic domain of cytoskeletal proteins such as talins, kindlins, 14-3-3 proteins, or filamins (Gahmberg *et al*, 2009). Such binding may promote dissociation of the α and β subunit TM domains, and integrin extension, in either model (Zhu *et al*, 2008; Ye *et al*, 2010) (Figure 7B and C). However, because of substantial flexibility in integrin leg domains, particularly at the interfaces between the I-EGF1 and I-EGF2 domains, and between the I-EGF4 and β-tail domains (Takagi *et al*, 2002; Nishida *et al*, 2006; Shi *et al*, 2007; Zhu *et al*, 2008; Chen *et al*, 2010; Xie *et al*, 2010) separation of the α and β subunit TM domains does not favour the open over the closed headpiece, as has been verified with integrin ectodomain preparations

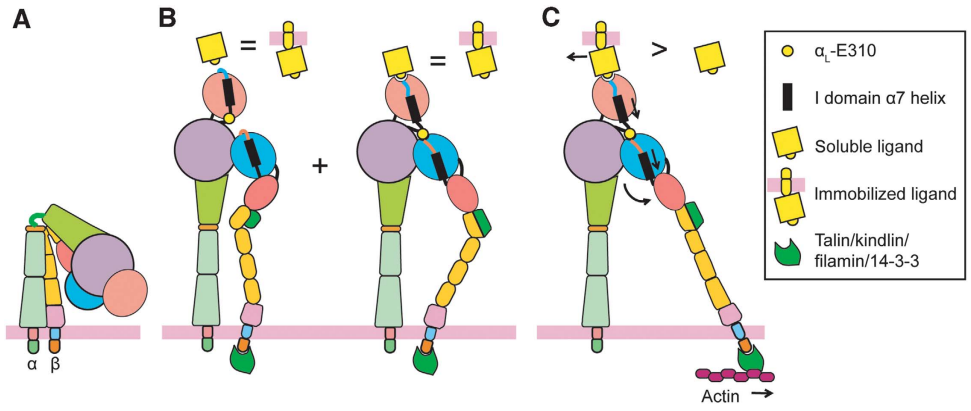

Figure 7 Models of integrin activation by inside–out signalling. (**A**) An inactive bent integrin. (**B**) The integrin is activated by protein binding to the β cytoplasmic tail, disrupting TM domain association and inducing an extended conformation with a closed or open headpiece. This model proposes equal binding affinity ('=') of soluble or immobilized ligand. (**C**) The translational motion or traction force model suggests that disruption of the TM domain association by cytoskeletal proteins can induce integrin extension, but fails to induce the open headpiece conformation due to considerable flexibility between integrin leg domains. This model proposes that the actin cytoskeleton induces translational motion. When immobilized ligand binds integrin, it resists translation, and force increases (arrows). Force is on pathway with hybrid domain swing out. Force thus acts as an allosteric effector by straightening the β leg, and pulling on the hybrid domain to swing it out. This model predicts substantially higher integrin affinity ('>') for ligand on substrates than in solution phase.

(Takagi *et al*, 2002; Nishida *et al*, 2006; Shi *et al*, 2007; Chen *et al*, 2010) (Figure 7B). Thus, leg separation in the absence of further events provides no structural mechanism for inducing the high affinity, open integrin headpiece state in response to intracellular signals. However, further events are provided by the translational motion or traction model, that notes that cytoskeletal proteins that bind integrins are associated with the actin cytoskeleton, which induces translational motion (Figure 7C). Once ligand is bound on the substrate, it will resist integrin translation, increase the force on and rigidify the β-leg domain, and provide a mechanism for transmission of allostery through otherwise flexible domains (Zhu *et al*, 2008).

Direct evidence for a translational motion/traction force model has yet to be found; however, other findings are consistent with it. Fluorescent microscopy of immunological synapses demonstrate rapid centripetal movement of actin filaments that correlate with centripetal LFA-1/ICAM-1 complex movement, precisely in the peripheral zone of the synapse where LFA-1 accumulates and functions in immunological synapses (Kaizuka *et al*, 2007). Moreover, rendering ICAM-1 and ICAM-2 highly mobile on target cells prevents proper lytic granule polarization and conjugate formation, while reducing lateral mobility of ICAM-2 on target cells enhances polarization and LFA-1-dependent adhesion (Gross *et al*, 2010).

The comprehensive set of monomeric affinity measurements reported here represent major advances in our understanding of both the basal and activated integrin states. They demonstrate that the integrin cell adhesion machinery distinguishes between soluble and substrate-bound ligand, resulting in a 300-fold increase in affinity between the primed and high affinity states. Recent studies on NK cells further suggest that LFA-1 can discriminate between ICAMs that are more or less resistant to applied force (Gross *et al*, 2010). Such distinctions may contribute to appropriate strengthening or disassembly of integrin adhesion sites, efficient traction in cell migration, and centring on antigen-bearing cells in the formation of immunological synapses.

Materials and methods

Reagents

PMA was from Calbiochem. BIRT377, XVA143, and compound #4 were as described (Last-Barney *et al*, 2001; Gadek *et al*, 2002; Shimaoka *et al*, 2003a). 2-Deoxy-D-glucose was from Sigma (St Louis, MO).

Antibodies

Monoclonal antibodies TS1/22, TS1/18, CBR LFA-1/2, KIM127, MEM148, m24, M1/70, and OKT3 have been described (Kung *et al*, 1979; Springer *et al*, 1979; Sanchez-Madrid *et al*, 1982; Dransfield and Hogg, 1989; Robinson *et al*, 1992; Petruzzelli *et al*, 1995; Drbal *et al*, 2001). Mouse $IgG_{2a}\kappa$ and goat anti-mouse IgG_{2a} were from Sigma, and sodium azide was removed by ultrafiltration.

Antibody fragmentation

Fab fragments were generated by digesting purified IgG with soluble papain (Calbiochem, Gibbstown, NJ). After inactivation of papain by iodoacetamide, Fc fragments were removed by protein A agarose (Pierce, Rockford, IL) and Fab purified by gel filtration on a Superdex 200 column (GE Healthcare, Piscataway, NJ).

Cell culture

293S cells with a dysfunctional *N*-acetyl glucosaminyl transferase I ($GnTI^-$) and K562 transfectants expressing wt or mutant LFA-1 have been described (Lu and Springer, 1997; Lu *et al*, 2001c; Reeves *et al*, 2002). A high affinity-conferring αI domain double-mutation (F265S/F292A; Jin *et al*, 2006) was introduced by overlap-extension PCR. K562 cells were stably transfected with F265S/F292A-α_L and wt β_2. Peripheral blood mononuclear cells were purified by Histopaque-1077 (Sigma) density centrifugation. Peripheral naive T lymphocytes were obtained by removal of non-T cells using the MACS Pan T-cell Isolation Kit (Miltenyi Biotech, Auburn, CA) following the manufacturer's instructions. These cells were 95% $CD3^+$ and were used within 4 h. To obtain IL-15-cultured T lymphocytes, lymphocytes were cultured in the presence of PHA (1 μg/ml) for 3 days followed by culture in 10 ng/ml IL-15 for 3–7 days. Depletion of metabolic energy was by pretreatment for 1 h at 37 °C with 50 mM 2-deoxy-D-glucose (Sigma) and 10 mM sodium azide.

Hi3-ICAM-1 expression and purification

DNA encoding the extracellular part of Hi3-ICAM-1 (Song *et al*, 2006) was ligated into the *Bsm*BI site of the ExpressTag-8 (ET-8) vector, which provided an N-terminal mouse immunoglobulin κ chain signal peptide and a C-terminal Gly–Gly–Gly linker followed by a hexahistidine tag. The Hi3-ICAM-1-coding sequence is

followed by an internal ribosome entry site that permits bicistronic expression of EGFP. Stably transfected 293S GnTI$^-$ cells were selected with 1 mg/ml G418 and enriched by two rounds of cell sorting for the top 2.5% EGFP expressers. The best Hi3-ICAM-1-expressing clones were identified by ELISA, and clone 10E10 was selected for Hi3-ICAM-1 expression in serum-free ExCell 293 SFM (Sigma) supplemented with 6 mM glutamine, 1 mg/ml G418, and 50 μg/ml gentamicin. Conditioned cell supernatant was harvested when cell viability was <50% and the protein purified on NiNTA agarose followed by Mono Q anion exchange chromatography. Fractions containing monomeric Hi3-ICAM-1 were identified by nonreducing SDS–PAGE, pooled, and concentrated. The cell line typically yielded 20–30 mg monomeric protein per litre cell culture supernatant.

Wild-type ICAM-1 expression and purification

Wt ICAM-1 (D1–D5) was fused to the same signal peptide and C-terminal linker with His-tag as Hi3-ICAM-1. This construct was cloned into the pLEXm vector (Aricescu *et al*, 2006) and expressed by transient transfection of 293S GnTI$^-$ cells. The cells were grown for 5 days in ExCell 293 SFM with 6 mM glutamine and gentamicin (50 μg/ml). The protein was purified on NiNTA agarose and frozen at −80 °C until use. Typical yields were 5–10 mg protein per litre.

Protein radioiodination

In a glass tube coated with 10 μg Iodogen (Pierce), 150 μg of TS1/22 Fab or 250 μg Hi3-ICAM-1 in 25 mM Tris pH 8.0, 400 mM NaCl was reacted with 500 μCi $Na^{125}I$ for 20 min at room temperature. The reaction was quenched with 2 mg/ml L-tyrosine for 5 min. After supplementation with 5 mM potassium iodide, the radioligand was purified on a PD-10 column (GE Healthcare) equilibrated with HBS (20 mM HEPES pH 7.4, 150 mM NaCl). Radioligand concentrations were determined by BCA using BSA as protein standard for ^{125}I-TS1/22 Fab or Hi3-ICAM-1 for ^{125}I-Hi3-ICAM-1. Specific activities were quantified with a Wizard 1470 automatic γ counter (Perkin-Elmer, Waltham, MA) and typically reached 150–250 Ci/mmol. BSA was added to a final concentration of 10 mg/ml and the radioligand was stored at −80 °C until use. Radioactivity was routinely >95% TCA-precipitable.

Saturation radioligand-binding assay

Cells were washed in binding buffer (L15 medium pH 7.4 with 1% BSA) and resuspended at 10^7 cells/ml. Aliquots of 10 μl (10^5 cells) were mixed in 0.6 ml microtubes with the same volume of binding buffer containing increasing concentrations of radioligand and incubated for 2 h at 37 °C. The cells were centrifuged through 150 μl dibutylphthalate:dioctylphthalate (2:1 v/v) to separate cell associated from unbound ligand. The tubes were frozen on dry ice and tips containing cell pellets were cut and analysed in a γ counter. Nonspecific binding of ^{125}I-TS1/22 Fab or ^{125}I-Hi3-ICAM-1 was determined in the presence of 150 μg/ml TS1/22 IgG or 10 mM EDTA, respectively, and subtracted from total binding. TS1/22 Fab binding reaches equilibrium after 2 h (Supplementary Figure S6). Potential receptor internalization was tested by washing cells after the incubation step with 50 mM glycine pH 2.8, 150 mM NaCl. Residual cell-associated ^{125}I-TS1/22 Fab was less than the subtracted nonspecifically associated Fab.

Competitive radioligand-binding assay

Cells (10^7 cells/ml) in binding buffer (L15 medium pH 7.4 with 1% BSA) with or without activators or inhibitors were aliquoted on ice (10^5 cells in 10 μl) in 0.6 ml microcentrifuge tubes, mixed with equal volumes of 20 nM ^{125}I-TS1/22 Fab containing increasing concentrations of Hi3-ICAM-1, and incubated for 2 h at 37 °C to allow activation or inhibition of LFA-1 and ligand binding at the same time. Activating or inhibiting Fab fragments were used at 20 μg/ml each, except TS1/18 (50 μg/ml). Chemokine activation was with 100 nM SDF-1α (R&D Systems). Activation by TCR crosslinking was as described (Dustin and Springer, 1989) by incubating cells with 20 μg/ml OKT3 (anti-CD3ε) antibody on ice and extensive washing at 4 °C. TCR were crosslinked by 2 μg/ml goat anti-mouse IgG_{2a} during ligand binding. For integrin activation by Mn^{2+}, cells were first washed with HEPES-buffered saline, pH 7.4 with 1% BSA (HBS/BSA) containing 10 mM EDTA followed by two washes in HBS/BSA. LFA-1 was activated with 1 mM Mn^{2+} in HBS/BSA. PMA was used at 1 μM, BIRT377 was 20 μM, XVA143 was 10 μM, compound #4 was 5 μM. Separation of cell-bound radioligand from free ligand and quantification was as described above. Nonspecific ^{125}I-TS1/22 Fab binding was determined in the presence of 100 μg/ml TS1/22 IgG and subtracted from total Fab binding to obtain specific binding. Specific Fab binding in the absence of Hi3-ICAM-1 competitor was set to 100% binding. Potential LFA-1 internalization was tested by acid washing T lymphocytes after incubation in the absence of competitor with 50 mM glycine, pH 2.8, 150 mM NaCl and measuring remaining cell-associated radioactivity. In all cases, the radioactivity that remained cell-bound after acid washing was equal or less than the subtracted nonspecifically bound ^{125}I-TS1/22 Fab and was not further considered.

Nonlinear regression analysis

Binding data were analysed by nonlinear regression analysis using the Levenberg–Marquardt method with Prism 5.03 for Windows (Graphpad, San Diego). Saturation binding data from total and nonspecific binding were globally fit to a one-site binding model extended by a nonspecific binding term (NS × [ligand]) (1) and best-fit curves were calculated.

$$\text{Bound} = \frac{B_{\max} \times [\text{ligand}]}{K_D + [\text{ligand}]} + \text{NS} \times [\text{ligand}] \quad (1)$$

Specific competition binding data were fit to one-site (equations 2 and 3) and two-site binding models (equations 4–6). $K_{D,Fab}$ was the affinity of the TS1/22 Fab for LFA-1 (24.38 nM), [Fab] was the TS1/22 Fab concentration used (10 nM), and B_0 was the specific TS1/22 Fab binding in the absence of competitor (not constrained for fitting). An extra sum-of-squares F-test was performed in Prism to compare fits to the one-site and two-site binding models. For $P<0.05$, the two-site binding model was accepted and P values are shown.

$$\text{Bound} = \frac{B_0}{1 + 10^{\log[\text{ICAM1}] - \log \text{IC}_{50}}} \quad (2)$$

$$\log \text{IC}_{50} = \log\left(10^{\log K_D \times \left(1 + \frac{[\text{Fab}]}{K_{D,\text{Fab}}}\right)}\right) \quad (3)$$

$$\text{Bound(site 1)} = \frac{[\text{Fab}] \times B_0}{[\text{Fab}] + K_{D,\text{Fab}} \times (1 + \frac{[\text{ICAM1}]}{10^{\log K_{D,\text{high}}}})} \quad (4)$$

$$\text{Bound(site 2)} = \frac{[\text{Fab}] \times B_0}{[\text{Fab}] + K_{D,\text{Fab}} \times (1 + \frac{[\text{ICAM1}]}{10^{\log K_{D,\text{low}}}})} \quad (5)$$

$$\text{Bound} = \text{bound(site 1)} \times \text{f(high)} + \text{bound(site 2)} \times (1 - \text{f(high)}) \quad (6)$$

The log K_D values were converted into K_D values and are given together with the ±1 s.e. intervals. To decide whether LFA-1 affinities in treated cells were significantly different from control cells, fits with log K_D parameter shared among data sets were compared to fits with individually fitted log K_D values by extra sum-of-squares F-tests in Prism software. Affinities were assumed to be significantly different if $P<0.05$.

Cell adhesion assay

Soluble ICAM-1 (D1–D5) was used to coat flat-bottom 96-well plates at 5 μg/ml for SKW3 cells and 10 μg/ml for cultured T lymphocytes. After coating, wells were blocked with 1% heat-treated BSA. Cells were labelled with 2′,7′-bis-(2-carboxyethyl)-5-(and-6)-carboxyfluorescein, acetoxymethyl ester (BCECF-AM) (4 μg/ml) in HBS (20 mM HEPES pH 7.4, 140 mM NaCl, 5 mM KCl, 5.5 mM glucose), extensively washed, resuspended on ice with activators or inhibitors to 2×10^6 cells/ml in L15/1% BSA, and aliquoted (50 μl) into coated plates. Activation of lymphocytes was by immersing the plate bottom for 30 min into a 37° C water bath after a 1-min centrifugation step at 200 *g*. Activation by chemokine or TCR crosslinking was as described above and was terminated after 2 or 10 min, respectively, by adding 200 μl 3.7% formaldehyde in HBS. Mn^{2+} activation was as described for the competitive radioligand-binding assay. Unbound cells were washed off

manually with HBSS + Ca + Mg (Invitrogen) using a multichannel pipette, until binding to BSA-coated surfaces of stimulated cells reached <5% of input. Therefore, results with different activators in Figure 3A–D are not directly comparable. Cells activated by Mn^{2+} were washed with HBS supplemented with 1 mM Mn^{2+}. The percentage of adherent cells was calculated from fluorescence measurements before and after washes using a Fluoroskan Ascent Microplate Fluorometer (Thermo Scientific; Ex 485 nm/Em 538 nm). Adhesion to BSA-coated control wells was subtracted from adhesion to ICAM-1-coated wells.

Flow cytometry

Cells were washed and stained in L15/1% BSA with 1 μg/ml FITC-labelled KIM127, m24, or mouse IgG_1 control antibody in the presence or absence of integrin activators or inhibitors for 30 min at 37 °C. Analysis was performed on a FACScan flow cytometer (BD Biosciences).

Supplementary data

Supplementary data are available at *The EMBO Journal* Online (http://www.embojournal.org).

Acknowledgements

This work was supported by NIH Grant CA31798 and a fellowship from the Swiss National Science Foundation. We thank Dr M Robinson (Celltech, Slough, UK), Dr Nancy Hogg (Imperial Cancer Research Fund, London, UK), and Dr V Horejsi (Institute of Molecular Genetics, Prague) for providing KIM127, m24, and MEM148 antibodies, respectively. We acknowledge Dr Terence Kelly (Boehringer Ingelheim, Ridgeway, CT), Dr Paul Gillespie (Roche, Nutley, NJ), and Genentech (South San Francisco, CA) for providing BIRT377, XVA143, and compound #4, respectively. The expression vector pLEXm was obtained from Dr Y Jones, Oxford, UK. We thank Drs Xing Chen and Yamei Yu for help with Fab fragmentation, and Drs Chafen Lu and Motomu Shimaoka for critically reading the manuscript.

Author contributions: TS designed and carried out the experiments and wrote the manuscript. TAS designed the overall experimental approach, supervised experiments, and wrote the manuscript.

Conflict of interest

The authors declare that they have no conflict of interest.

References

Alonso JL, Essafi M, Xiong JP, Stehle T, Arnaout MA (2002) Does the integrin αA domain act as a ligand for its βA domain? *Curr Biol* **12:** R340–R342

Aricescu AR, Lu W, Jones EY (2006) A time- and cost-efficient system for high-level protein production in mammalian cells. *Acta Crystallogr D Biol Crystallogr* **62**(Part 10)**:** 1243–1250

Beglova N, Blacklow SC, Takagi J, Springer TA (2002) Cysteine-rich module structure reveals a fulcrum for integrin rearrangement upon activation. *Nat Struct Biol* **9:** 282–287

Bolomini-Vittori M, Montresor A, Giagulli C, Staunton D, Rossi B, Martinello M, Constantin G, Laudanna C (2009) Regulation of conformer-specific activation of the integrin LFA-1 by a chemokine-triggered Rho signaling module. *Nat Immunol* **10:** 185–194

Chen X, Xie C, Nishida N, Li Z, Walz T, Springer TA (2010) Requirement of open headpiece conformation for activation of leukocyte integrin $\alpha_X\beta_2$. *Proc Natl Acad Sci USA* **107:** 14727–14732

Constantin G, Majeed M, Giagulli C, Piccib L, Kim JY, Butcher EC, Laudanna C (2000) Chemokines trigger immediate β2 integrin affinity and mobility changes: differential regulation and roles in lymphocyte arrest under flow. *Immunity* **13:** 759–769

Dransfield I, Cabañas C, Craig A, Hogg N (1992) Divalent cation regulation of the function of the leukocyte integrin LFA-1. *J Cell Biol* **116:** 219–226

Dransfield I, Hogg N (1989) Regulated expression of Mg^{2+} binding epitope on leukocyte integrin alpha subunits. *EMBO J* **8:** 3759–3765

Drbal K, Angelisova P, Cerny J, Hilgert I, Horejsi V (2001) A novel anti-CD18mAb recognizes an activation-related epitope and induces a high-affinity conformation in leukocyte integrins. *Immunobiology* **203:** 687–698

Dustin ML, Bromley SK, Zhengyan K, Peterson DA, Unanue ER (1997) Antigen receptor engagement delivers a stop signal to migrating T lymphocytes. *Proc Natl Acad Sci USA* **94:** 3909–3913

Dustin ML, Springer TA (1989) T cell receptor cross-linking transiently stimulates adhesiveness through LFA-1. *Nature* **341:** 619–624

Emsley J, Knight CG, Farndale RW, Barnes MJ, Liddington RC (2000) Structural basis of collagen recognition by integrin $\alpha_2\beta_1$. *Cell* **101:** 47–56

Feigelson SW, Pasvolsky R, Cemerski S, Shulman Z, Grabovsky V, Ilani T, Sagiv A, Lemaitre F, Laudanna C, Shaw AS, Alon R (2010) Occupancy of lymphocyte LFA-1 by surface-immobilized ICAM-1 is critical for TCR- but not for chemokine-triggered LFA-1 conversion to an open headpiece high-affinity state. *J Immunol* **185:** 7394–7404

Gadek TR, Burdick DJ, McDowell RS, Stanley MS, Marsters Jr JC, Paris KJ, Oare DA, Reynolds ME, Ladner C, Zioncheck KA, Lee WP, Gribling P, Dennis MS, Skelton NJ, Tumas DB, Clark KR, Keating SM, Beresini MH, Tilley JW, Presta LG *et al* (2002) Generation of an LFA-1 antagonist by the transfer of the ICAM-1 immunoregulatory epitope to a small molecule. *Science* **295:** 1086–1089

Gahmberg CG, Fagerholm SC, Nurmi SM, Chavakis T (2009) Regulation of integrin activity and signalling. *Biochem Biophys Acta* **1790:** 431–444

Ganpule G, Knorr R, Miller JM, Carron CP, Dustin ML (1997) Low affinity of cell surface lymphocyte function-associated antigen-1 (LFA-1) generates selectivity for cell-cell interactions. *J Immunol* **159:** 2685–2692

Grakoui A, Bromley SK, Sumen C, Davis MM, Shaw AS, Allen PM, Dustin ML (1999) The immunological synapse: a molecular machine controlling T cell activation. *Science* **285:** 221–227

Gross CC, Brzostowski JA, Liu D, Long EO (2010) Tethering of intercellular adhesion molecule on target cells is required for LFA-1-dependent NK cell adhesion and granule polarization. *J Immunol* **185:** 2918–2926

Hibbs ML, Xu H, Stacker SA, Springer TA (1991) Regulation of adhesion to ICAM-1 by the cytoplasmic domain of LFA-1 integrin β subunit. *Science* **251:** 1611–1613

Humphries MJ (2000) Integrin structure. *Biochem Soc Trans* **28:** 311–339

Huth JR, Olejniczak ET, Mendoza R, Liang H, Harris EA, Lupher Jr ML, Wilson AE, Fesik SW, Staunton DE (2000) NMR and mutagenesis evidence for an I domain allosteric site that regulates lymphocyte function-associated antigen 1 ligand binding. *Proc Natl Acad Sci USA* **97:** 5231–5236

Jin M, Song G, Kim Y-S, Astrof N, Shimaoka M, Wittrup D, Springer TA (2006) Directed evolution to probe protein allostery and integrin I domains of 200 000-fold higher affinity. *Proc Natl Acad USA* **103:** 5758–5763

Kaizuka Y, Douglass AD, Varma R, Dustin ML, Vale RD (2007) Mechanisms for segregating T cell receptor and adhesion molecules during immunological synapse formation in Jurkat T cells. *Proc Natl Acad USA* **104:** 20296–20301

Kallen J, Welzenbach K, Ramage P, Geyl D, Kriwacki R, Legge G, Cottens S, Weitz-Schmidt G, Hommel U (1999) Structural basis for LFA-1 inhibition upon lovastatin binding to the CD11a I-domain. *J Mol Biol* **292:** 1–9

Kim M, Carman CV, Springer TA (2003) Bidirectional transmembrane signaling by cytoplasmic domain separation in integrins. *Science* **301:** 1720–1725

Kim M, Carman CV, Yang W, Salas A, Springer TA (2004) The primacy of affinity over clustering in regulation of adhesiveness of the integrin $\alpha_L\beta_2$. *J Cell Biol* **167:** 1241–1253

Kucik DF, Dustin ML, Miller JM, Brown EJ (1996) Adhesion-activating phorbol ester increases the mobility of leukocyte integrin LFA-1 in cultured lymphocytes. *J Clin Invest* **97:** 2139–2144

Kung PC, Goldstein G, Reinherz EL, Schlossman SF (1979) Monoclonal antibodies defining distinctive human T cell surface antigens. *Science NY* **206:** 347–349

Last-Barney K, Davidson W, Cardozo M, Frye LL, Grygon CA, Hopkins JL, Jeanfavre DD, Pav S, Qian C, Stevenson JM, Tong L, Zindell R, Kelly TA (2001) Binding site elucidation of hydantoin-based antagonists of LFA-1 using multidisciplinary technologies: evidence for the allosteric inhibition of a protein-protein interaction. *J Am Chem Soc* **123:** 5643–5650

Lau TL, Kim C, Ginsberg MH, Ulmer TS (2009) The structure of the integrin $\alpha_{IIb}\beta_3$ transmembrane complex explains integrin transmembrane signalling. *EMBO J* **9:** 1351–1361

Lee J-O, Rieu P, Arnaout MA, Liddington R (1995) Crystal structure of the A domain from the α subunit of integrin CR3 (CD11b/CD18). *Cell* **80:** 631–638

Li YF, Tang RH, Puan KJ, Law SK, Tan SM (2007) The cytosolic protein talin induces an intermediate affinity integrin $\alpha_L\beta_2$. *J Biol Chem* **282:** 24310–24319

Lollo BA, Chan KW, Hanson EM, Moy VT, Brian AA (1993) Direct evidence for two affinity states for lymphocyte function-associated antigen 1 on activated T cells. *J Biol Chem* **268:** 21693–21700

Lu C, Ferzly M, Takagi J, Springer TA (2001a) Epitope mapping of antibodies to the C-terminal region of the integrin β2 subunit reveals regions that become exposed upon receptor activation. *J Immunol* **166:** 5629–5637

Lu C, Shimaoka M, Ferzly M, Oxvig C, Takagi J, Springer TA (2001b) An isolated, surface-expressed I domain of the integrin $\alpha_L\beta_2$ is sufficient for strong adhesive function when locked in the open conformation with a disulfide. *Proc Natl Acad Sci USA* **98:** 2387–2392

Lu C, Shimaoka M, Salas A, Springer TA (2004) The binding sites for competitive antagonistic, allosteric antagonistic, and agonistic antibodies to the I domain of integrin LFA-1. *J Immunol* **173:** 3972–3978

Lu C, Shimaoka M, Zang Q, Takagi J, Springer TA (2001c) Locking in alternate conformations of the integrin $\alpha_L\beta_2$ I domain with disulfide bonds reveals functional relationships among integrin domains. *Proc Natl Acad Sci USA* **98:** 2393–2398

Lu C, Springer TA (1997) The alpha subunit cytoplasmic domain regulates the assembly and adhesiveness of integrin lymphocyte function-associated antigen-1 (LFA-1). *J Immunol* **159:** 268–278

Lub M, van Vliet SJ, Oomen SP, Pieters RA, Robinson M, Figdor CG, van Kooyk Y (1997) Cytoplasmic tails of beta1, beta2, and beta7 integrins differentially regulate LFA-1 function in K562 cells. *Mol Biol Cell* **8:** 719–728

Luo B-H, Carman CV, Springer TA (2007) Structural basis of integrin regulation and signaling. *Annu Rev Immunol* **25:** 619–647

Mempel TR, Henrickson SE, Von Andrian UH (2004) T-cell priming by dendritic cells in lymph nodes occurs in three distinct phases. *Nature* **427:** 154–159

Moser M, Legate KR, Zent R, Fassler R (2009) The tail of integrins, Talin and Kindlins. *Science* **234:** 895–899

Nishida N, Xie C, Shimaoka M, Cheng Y, Walz T, Springer TA (2006) Activation of leukocyte β_2 integrins by conversion from bent to extended conformations. *Immunity* **25:** 583–594

Petruzzelli L, Maduzia L, Springer TA (1995) Activation of LFA-1 (CD11a/CD18) and Mac-1 (CD11b/CD18) mimicked by an antibody directed against CD18. *J Immunol* **155:** 854–866

Reeves PJ, Callewaert N, Contreras R, Khorana HG (2002) Structure and function in rhodopsin: high-level expression of rhodopsin with restricted and homogeneous N-glycosylation by a tetracycline-inducible N-acetylglucosaminyltransferase I-negative HEK293S stable mammalian cell line. *Proc Natl Acad Sci USA* **99:** 13419–13424

Robinson MK, Andrew D, Rosen H, Brown D, Ortlepp S, Stephens P, Butcher EC (1992) Antibody against the Leu-cam β-chain (CD18) promotes both LFA-1-and CR3-dependent adhesion events. *J Immunol* **148:** 1080–1085

Salas A, Shimaoka M, Kogan AN, Harwood C, von Andrian UH, Springer TA (2004) Rolling adhesion through an extended conformation of integrin $\alpha_L\beta_2$ and relation to α I and β I-like domain interaction. *Immunity* **20:** 393–406

Sanchez-Madrid F, Krensky AM, Ware CF, Robbins E, Strominger JL, Burakoff SJ, Springer TA (1982) Three distinct antigens associated with human T lymphocyte-mediated cytolysis: LFA-1, LFA-2, and LFA-3. *Proc Natl Acad Sci USA* **79:** 7489–7493

Shamri R, Grabovsky V, Gauguet JM, Feigelson S, Manevich E, Kolanus W, Robinson MK, Staunton DE, von Andrian UH, Alon R (2005) Lymphocyte arrest requires instantaneous induction of an extended LFA-1 conformation mediated by endothelium-bound chemokines. *Nat Immunol* **6:** 497–506

Shi M, Foo SY, Tan SM, Mitchell EP, Law SK, Lescar J (2007) A structural hypothesis for the transition between bent and extended conformations of the leukocyte β2 integrins. *J Biol Chem* **282:** 30198–30206

Shi M, Sundramurthy K, Liu B, Tan SM, Law SK, Lescar J (2005) The crystal structure of the plexin-semaphorin-integrin domain/hybrid domain/I-EGF1 segment from the human integrin β2 subunit at 1.8-A resolution. *J Biol Chem* **280:** 30586–30593

Shimaoka M, Kim M, Cohen EH, Yang W, Astrof N, Peer D, Salas A, Ferrand A, Springer TA (2006) AL-57, a ligand-mimetic antibody to integrin LFA-1, reveals chemokine-induced affinity upregulation in lymphocytes. *Proc Natl Acad Sci USA* **103:** 13991–13996

Shimaoka M, Lu C, Palframan R, von Andrian UH, Takagi J, Springer TA (2001) Reversibly locking a protein fold in an active conformation with a disulfide bond: integrin αL I domains with high affinity and antagonist activity *in vivo*. *Proc Natl Acad Sci USA* **98:** 6009–6014

Shimaoka M, Salas A, Yang W, Weitz-Schmidt G, Springer TA (2003a) Small molecule integrin antagonists that bind to the β2 subunit I-like domain and activate signals in one direction and block them in another. *Immunity* **19:** 391–402

Shimaoka M, Springer TA (2003) Therapeutic antagonists and the conformational regulation of integrin structure and function. *Nat Rev Drug Disc* **2:** 703–716

Shimaoka M, Xiao T, Liu J-H, Yang Y, Dong Y, Jun C-D, McCormack A, Zhang R, Joachimiak A, Takagi J, Wang J-h, Springer TA (2003b) Structures of the αL I domain and its complex with ICAM-1 reveal a shape-shifting pathway for integrin regulation. *Cell* **112:** 99–111

Shulman Z, Shinder V, Klein E, Grabovsky V, Yeger O, Geron E, Montresor A, Bolomini-Vittori M, Feigelson SW, Kirchhausen T, Laudanna C, Shakhar G, Alon R (2009) Lymphocyte crawling and transendothelial migration require chemokine triggering of high-affinity LFA-1 integrin. *Immunity* **30:** 384–396

Song G, Lazar GA, Kortemme T, Shimaoka M, Desjarlais JR, Baker D, Springer TA (2006) Rational design of ICAM-1 variants for antagonizing integrin LFA-1-dependent adhesion. *J Biol Chem* **281:** 5042–5049

Springer TA, Galfre G, Secher DS, Milstein C (1979) Mac-1: a macrophage differentiation antigen identified by monoclonal antibody. *Eur J Immunol* **9:** 301–306

Stanley P, Smith A, McDowall A, Nicol A, Zicha D, Hogg N (2008) Intermediate-affinity LFA-1 binds alpha-actinin-1 to control migration at the leading edge of the T cell. *EMBO J* **27:** 62–75

Stewart MP, Cabanas C, Hogg N (1996) T cell adhesion to intercellular adhesion molecule-1 (ICAM-1) is controlled by cell spreading and the activation of integrin LFA-1. *J Immunol* **156:** 1810–1817

Takagi J, Petre BM, Walz T, Springer TA (2002) Global conformational rearrangements in integrin extracellular domains in outside-in and inside-out signaling. *Cell* **110:** 599–611

Tang RH, Tng E, Law SK, Tan SM (2005) Epitope mapping of monoclonal antibody to integrin $\alpha_L\beta_2$ hybrid domain suggests different requirements of affinity states for intercellular adhesion molecules (ICAM)-1 and ICAM-3 binding. *J Biol Chem* **280:** 29208–29216

Tang XY, Li YF, Tan SM (2008) Intercellular adhesion molecule-3 binding of integrin $\alpha_L\beta_2$ requires both extension and opening of the integrin headpiece. *J Immunol* **180:** 4793–4804

van Kooyk Y, van Vliet SJ, Figdor CG (1999) The actin cytoskeleton regulates LFA-1 ligand binding through avidity rather than affinity changes. *J Biol Chem* **274:** 26869–26877

Wegener KL, Partridge AW, Han J, Pickford AR, Liddington RC, Ginsberg MH, Campbell ID (2007) Structural basis of integrin activation by talin. *Cell* **128:** 171–182

Weitz-Schmidt G, Welzenbach K, Brinkmann V, Kamata T, Kallen J, Bruns C, Cottens S, Takada Y, Hommel U (2001) Statins selectively inhibit leukocyte function antigen-1 by binding to a novel regulatory integrin site. *Nat Med* **7:** 687–692

Xiao T, Takagi J, Wang J-h, Coller BS, Springer TA (2004) Structural basis for allostery in integrins and binding of fibrinogen-mimetic therapeutics. *Nature* **432:** 59–67

Xie C, Zhu J, Chen X, Mi L, Nishida N, Springer TA (2010) Structure of an integrin with an α I domain, complement receptor type 4. *EMBO J* **29:** 666–679

Xiong J-P, Stehle T, Diefenbach B, Zhang R, Dunker R, Scott DL, Joachimiak A, Goodman SL, Arnaout MA (2001) Crystal structure of the extracellular segment of integrin $\alpha_V\beta_3$. *Science* **294:** 339–345

Yang W, Carman CV, Kim M, Salas A, Shimaoka M, Springer TA (2006) A small molecule agonist of an integrin, $\alpha_L\beta_2$. *J Biol Chem* **281:** 37904–37912

Yang W, Shimaoka M, Salas A, Takagi J, Springer TA (2004) Intersubunit signal transmission in integrins by a receptor-like interaction with a pull spring. *Proc Natl Acad Sci USA* **101:** 2906–2911

Ye F, Hu G, Taylor D, Ratnikov B, Bobkov AA, McLean MA, Sligar SG, Taylor KA, Ginsberg MH (2010) Recreation of the terminal events in physiological integrin activation. *J Biol Chem* **188:** 157–173

Zhu J, Luo BH, Barth P, Schonbrun J, Baker D, Springer TA (2009) The structure of a receptor with two associating transmembrane domains on the cell surface: integrin $\alpha_{IIb}\beta_3$. *Mol Cell* **34:** 234–249

Zhu J, Luo BH, Xiao T, Zhang C, Nishida N, Springer TA (2008) Structure of a complete integrin ectodomain in a physiologic resting state and activation and deactivation by applied forces. *Mol Cell* **32:** 849–861

Figure S1. A. Saturation binding of ^{125}I-TS1/22 Fab to LFA-1 on cultured T lymphocytes activated by CBR LFA-1/2+KIM127+MEM148 Fab. Data are averages±SE from two independent experiments in triplicates. Curve is best fit to specific binding model and derived $K_{D,Fab}$ is shown ±SE. B,D. Competition binding of Hi3-ICAM-1 to freshly isolated naïve T lymphocytes before (B) or after activation by SDF-1α (D). Averages±SE are from triplicate determination. Best fit curves and K_D values with 1 SE intervals are shown. Affinities were compared by F-test with indicated p value. C. Adhesion of K562 transfectants expressing wt LFA-1 or high affinity LFA-1 to ICAM-1 substrate in the presence of 1 mM Ca^{2+}/1 mM Mg^{2+} or 10 mM EDTA. Averages±SE are from triplicate determinations.

Figure S2. A-C. Hi3-ICAM-1 competition binding to T lymphocytes activated by PMA (A), SDF-1α (B), or T cell receptor crosslinking with OKT3 and anti-IgG_{2a} (C). Data is from Fig. 3E-G. Data analysis was as in Fig. 3, except that the top of the curve (B_0) was constrained to 100% during nonlinear regression.

Figure S3. The TS1/18 Fab allosterically inhibits LFA-1 adhesiveness induced by CBR LFA-1/2+KIM127. Adhesion of T lymphocytes to ICAM-1 substrate was measured without (left) or after activation by CBR LFA-1/2+KIM127 Fab (right) as a function of concentration of TS1/18 Fab. Averages±SE from triplicates.

Figure S4. ^{125}I-Hi3-ICAM-1 saturation binding to LFA-1 on T lymphocytes activated by Fab combination. Averages±SE are from two independent triplicate experiments. Curve is best fit to specific binding model and calculated K_D±SE is shown.

Figure S5. Induction of high affinity LFA-1 by KIM127 Fab is not detectable at 0 °C. T lymphocytes were activated by Fab at 37 °C and then transferred to ice for competition binding assays. A. Control LFA-1 has low affinity for ligand. B. KIM127 Fab induces LFA-1 priming in the absence of detectable high affinity receptors, whereas the combination of CBR LFA-1/2 and KIM127 Fab induces high affinity binding of ligand (C). Averages±SE from 1 to 8 experiments, each performed in triplicate.

Figure S6. Binding kinetics of TS1/22 Fab. K562 transfectants expressing LFA-1 were incubated with 10 nM ^{125}I-TS1/22 Fab for various time at 37 °C, and specific binding was determined as described in the experimental section. Averages±SE from triplicates.

Figure S1

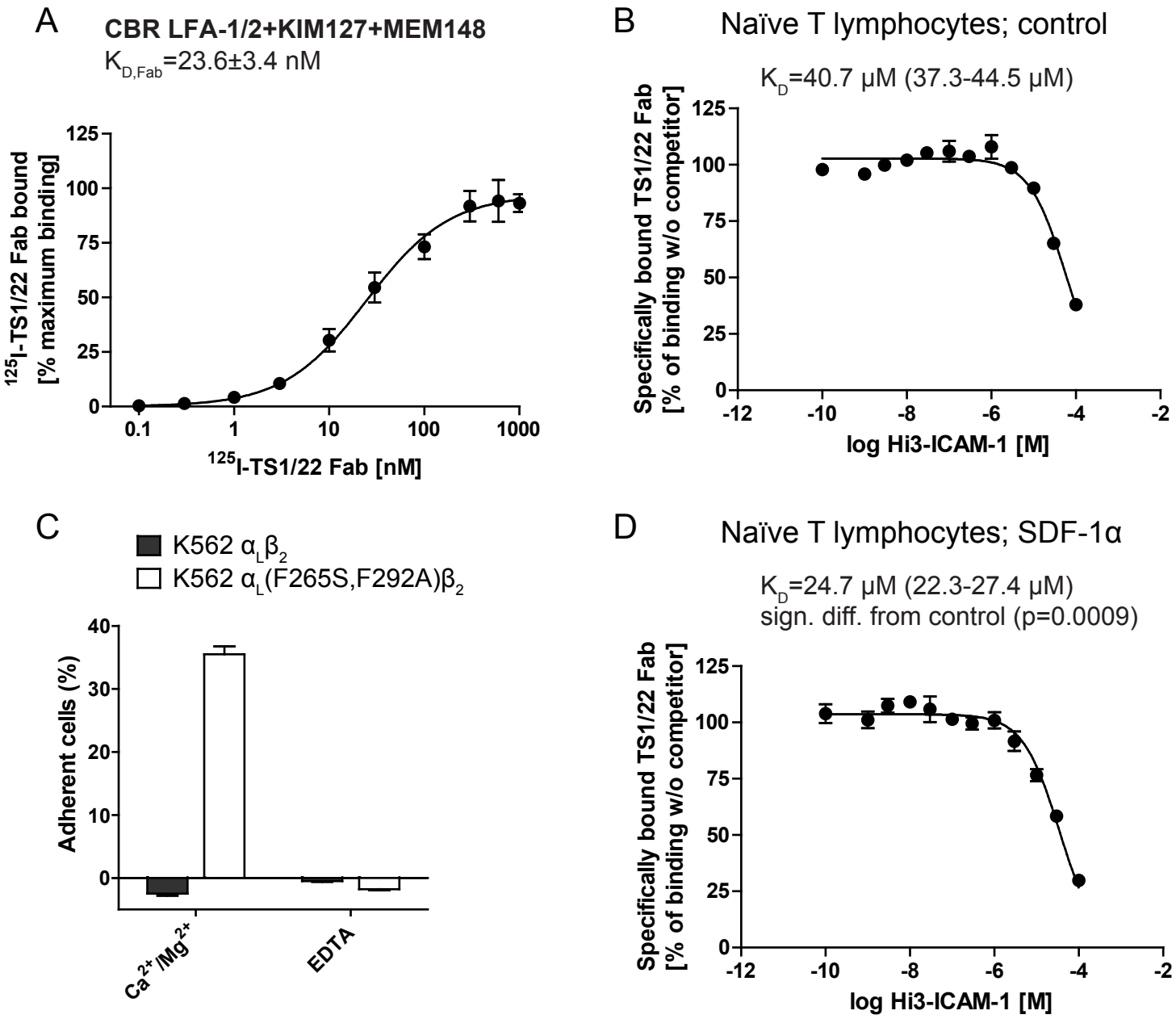
A
CBR LFA-1/2+KIM127+MEM148
$K_{D,Fab}$=23.6±3.4 nM
^{125}I-TS1/22 Fab bound [% maximum binding]
^{125}I-TS1/22 Fab [nM]
B
Naïve T lymphocytes; control
K_D=40.7 µM (37.3-44.5 µM)
Specifically bound TS1/22 Fab [% of binding w/o competitor]
log Hi3-ICAM-1 [M]
C
K562 $\alpha_L\beta_2$
K562 α_L(F265S,F292A)β_2
Adherent cells (%)
Ca^{2+}/Mg^{2+}
EDTA
D
Naïve T lymphocytes; SDF-1α
K_D=24.7 µM (22.3-27.4 µM)
sign. diff. from control (p=0.0009)
Specifically bound TS1/22 Fab [% of binding w/o competitor]
log Hi3-ICAM-1 [M]

Figure S2

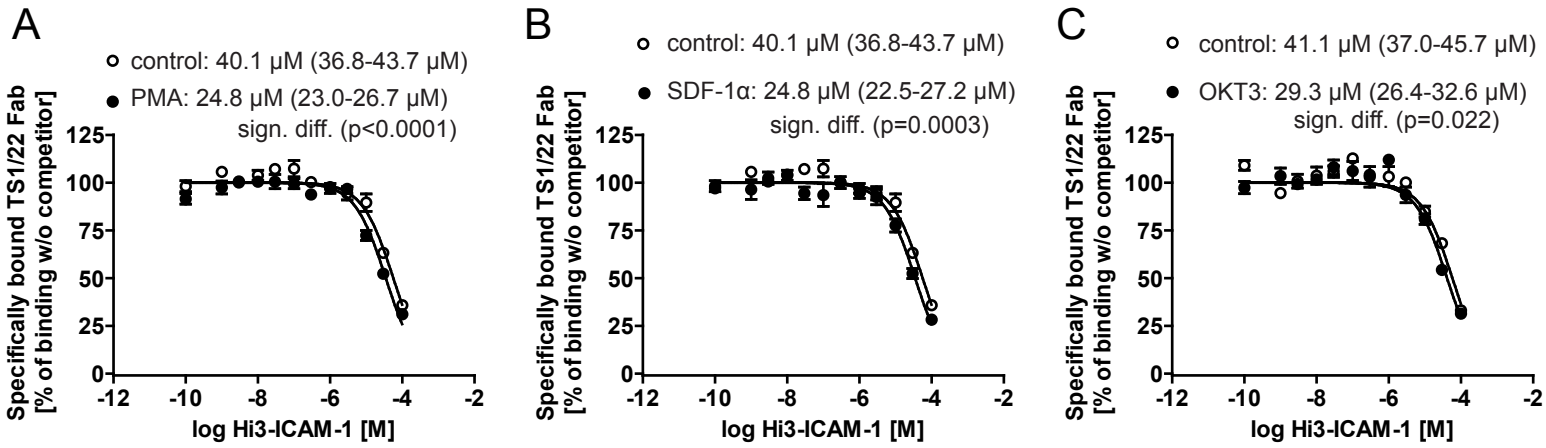
A
control: 40.1 µM (36.8-43.7 µM)
PMA: 24.8 µM (23.0-26.7 µM)
sign. diff. (p<0.0001)
Specifically bound TS1/22 Fab [% of binding w/o competitor]
log Hi3-ICAM-1 [M]
B
control: 40.1 µM (36.8-43.7 µM)
SDF-1α: 24.8 µM (22.5-27.2 µM)
sign. diff. (p=0.0003)
Specifically bound TS1/22 Fab [% of binding w/o competitor]
log Hi3-ICAM-1 [M]
C
control: 41.1 µM (37.0-45.7 µM)
OKT3: 29.3 µM (26.4-32.6 µM)
sign. diff. (p=0.022)
Specifically bound TS1/22 Fab [% of binding w/o competitor]
log Hi3-ICAM-1 [M]

Figure S3

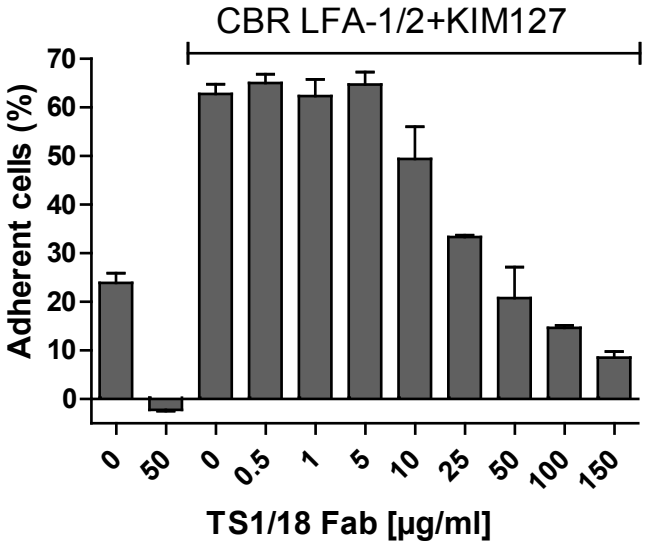
CBR LFA-1/2+KIM127
Adherent cells (%)
70
60
50
40
30
20
10
0
0
50
0
0.5
1
5
10
25
50
100
150
TS1/18 Fab [µg/ml]

Figure S4

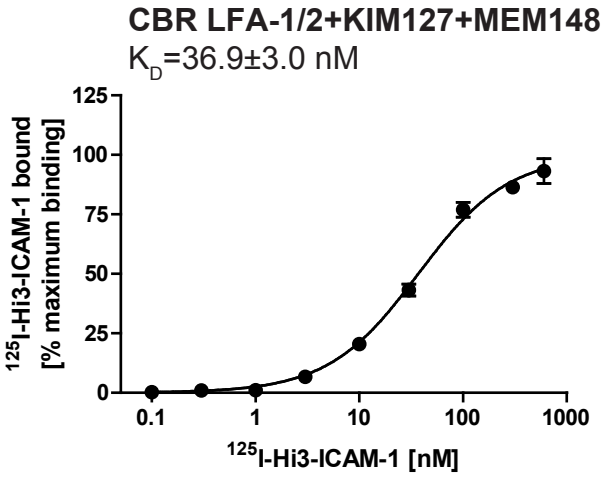
CBR LFA-1/2+KIM127+MEM148
K_D=36.9±3.0 nM
^{125}I-Hi3-ICAM-1 bound [% maximum binding]
125
100
75
50
25
0
0.1
1
10
100
1000
^{125}I-Hi3-ICAM-1 [nM]

Figure S5

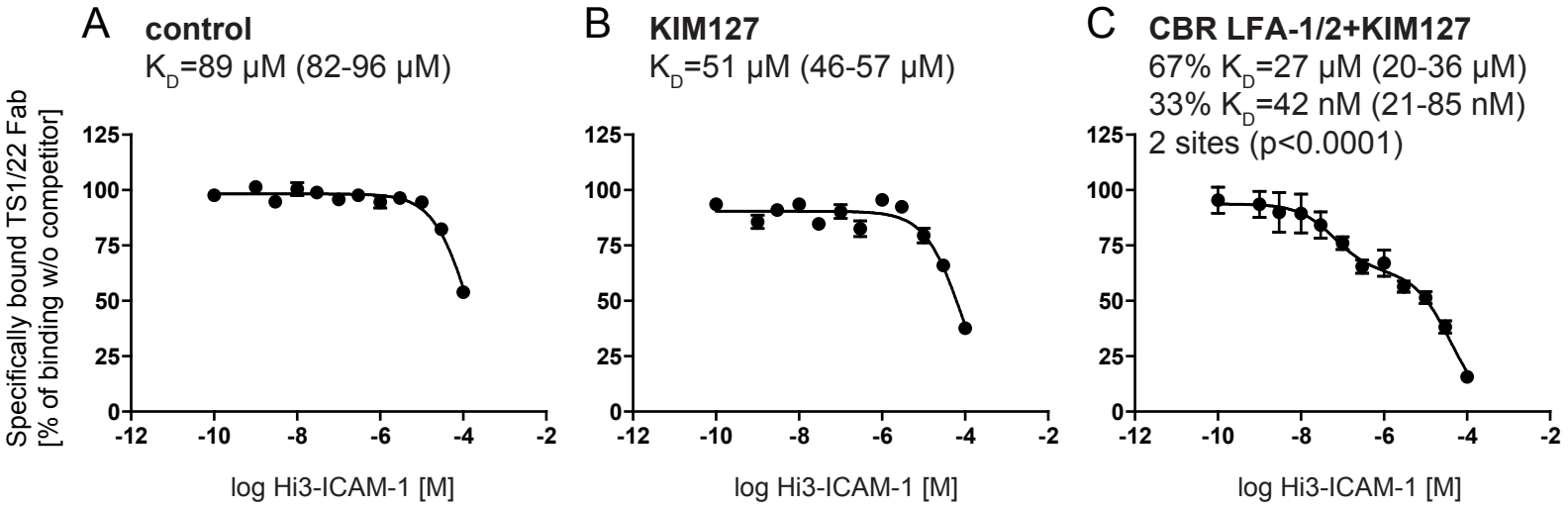
A
control
K_D=89 µM (82-96 µM)
B
KIM127
K_D=51 µM (46-57 µM)
C
CBR LFA-1/2+KIM127
67% K_D=27 µM (20-36 µM)
33% K_D=42 nM (21-85 nM)
2 sites (p<0.0001)
Specifically bound TS1/22 Fab
[% of binding w/o competitor]
125
100
75
50
25
0
-12
-10
-8
-6
-4
-2
log Hi3-ICAM-1 [M]

Figure S6

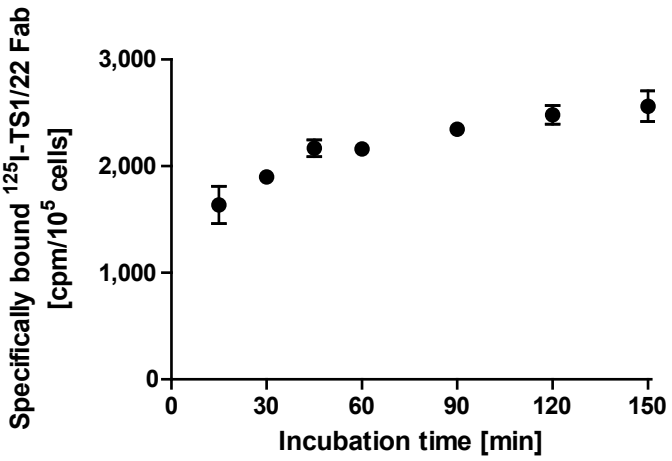
Specifically bound ^{125}I-TS1/22 Fab [cpm/10^5 cells]
3,000
2,000
1,000
0
0
30
60
90
120
150
Incubation time [min]